D4: Report on the investigation of the impact of contaminants in H2 and air contaminants on PEM Fuel Cell (FC) (reliability) and durability (sustainability) under short-term and long-term operation, including recommendations for air quality sensors needed for monitoring FC systems

Project	19ENG03 MefHySto
Due Date	2023/11/30
Release date	2024/01/29
Leading partner	CEA
Status	FINAL VERSION
Authors	NPL Jonathan Goh
	NPL Graham Smith
	CEA Fabrice Micoud
	CEA Sylvie Escribano
	CEA Sarah Fayolle
	CEA Gareth Keeley
	UDC Soledad Muniategui
	UDC Jose Andrade
	UDC Purificación López-Mahía
	UDC María Fernández-Amado

Dissemination level:

PU Public

PP Restricted to other programme participants

RE Restricted to a group specified by the consortium

CO Confidential, only for members of the consortium

EMPIR

EURAMET

The EMPIR initiative is co-funded by the European Union's Horizon 2020 research and innovation programme and the EMPIR Participating States

Document history

Version	Date	Description
1	29/01/2024	Released version

Table of contents

List of acronyms

ALPIX	Laboratory test bench for PEMFC system at CEA (1 kW)
ATD	Automated Thermal Desorber
ATIS	Adsorbent Tube Injector System
CEA	Commissariat à l'Énergie Atomique et aux Énergies Alternatives
EEA	European Environment Agency
IS	Internal Standard
ISO	International organization for standardization
ITEX-DHS	In-tube extraction dynamic headspace
GC	Gas chromatograph
GC-MS	Gas chromatography-mass spectrometry
HYDRAITE	Hydrogen Delivery Risk Assessment and Impurity Tolerance Evaluation, research project (FCH-JU now Clean Hydrogen, Grant agreement No 779475.)
LOD	Limit of detection
LOQ	Limit of quantitation
MetroHyVe	Metrology for hydrogen vehicles, EURAMET research project (16ENG01)
MetroHyVe2	Metrology for hydrogen vehicles 2, EURAMET research project (19ENG04)
PEMFC	Proton-exchange membrane fuel cell
PFSA	Perfluoroalkyl sulphonates
RH	Relative Humidity
RSD	Relative standard deviation
SENEPY	Hydrogen Experimental Platform at CEA
TD	Thermal desorption
UDC	Universidade da Coruña
VOCs	Volatile organic compounds
NMR	Nuclear Magnetic Resonance

1 Introduction

1.1 Purpose

This report documents the investigation of the impact of complex mixtures of impurities in hydrogen and air on PEMFC under short-term and long-term operation as carried out at NPL. This work was carried out at NPL with the assistance of CEA, UDC and Reganosa (while this company was involved in Mefhysto, before they left it) as part of WP3 of the MefHySto project and is a resume of the NPL's, CEA's and UDC's contributions to Deliverable 4. To the knowledge of the authors, this is one of the first instances where a complex mixture with more than three contaminants has been used to poison a fuel cell. As such, the work performed ostensibly represents a worst-case scenario of fuel cell poisoning on the basis of the ISO 14687:2019(D) standard which specifies the threshold limits for each contaminant in hydrogen for vehicular applications.

1.2 Accountabilities

The work package activities reported herein are shown in Table 1.

Table 1 - Summary of activities and accountabilities of tasks (P – Partner)

Activity number	Activity summary	CEA	NPL	UDC	Reganosa
Preparation of gas reference mixtures					
A3.1.1	Define the hydrogen and air gas mixtures to be considered, as well as their respective concentrations for PEM FC testing.	P	Lead	P	
A3.1.2	Select and supply FC components required for single cell testing.	Lead	P		
A3.1.3	Select and supply FC components required for short-stack cell testing.	Lead	P		
A3.1.4	Prepare 3 different gas mixtures of contaminants in hydrogen and 3 different gas mixtures of contaminants in air.	P	Lead	P	P
Evaluate and determine impact of contaminants in hydrogen supply on PEMFC performance					
A3.2.1	Conduct small scale electrochemical measurements to correlate with contamination process.	Lead	P		
A3.2.2	Test single cell PEMFC using hydrogen contaminant mixtures prepared in A3.1.4.	Lead	P		
A3.2.3	Test short-stack PEMFC under reference and polluted hydrogen conditions.	Lead	P		
Evaluate and determine impact of contaminants in air supply on PEMFC performance					
A3.3.1	Study rotating disk electrode	Lead	P		
A3.3.2	Test single cell PEMFC using air contaminant mixtures prepared in A3.1.4.	Lead	P		
A3.3.3	Recommendations for air quality analyses	Lead	P		
A3.3.4	Report on investigation from activities A3.1.x to A3.3.x i.e. this report.	P	P	P	P
Validate a metrological chain for gas analysis at a H_2 platform level					
A3.4.1	Preparation and adaptation of CEA's demonstration H_2 platform "SENEPY	Lead	P	P	P
A3.4.2	Validation of metrological chain	Lead	P	P	P
A3.4.3	Validation report of metrological chain	Lead	P	P	P

1.3 Scope

This work focused on low temperature PEMFCs, operating below 100 °C, investigating the impact of contaminants on the short-term performance and long-term durability. PEMFCs operate using a supply of hydrogen and oxygen (from air) and as such are highly sensitive to contaminants in both the hydrogen and air streams, which may reduce power, efficiency and/or lifetime of the PEMFC depending on several factors (type of contaminant and concentration, operating conditions etc.).

Previous studies of impurities' impact on fuel cells have focused on binary or ternary mixtures of contaminants and there has been no systematic study on the impact of a complex mixtures of impurities representing 'realistic' contamination scenarios. This study used a complex mixture of contaminants that reflect a worst-case, yet still permissible, scenario for fuel cell contamination. The test composition and concentration of the contaminants in hydrogen were selected based on the ISO 14687:2019(D) standard, and in consideration of the potential interaction of compounds when prepared in a cylinder. Air contaminants and concentrations were selected with real world averages[1] from the UK and EU as guidance to represent urban and suburban air quality. More details on prior work and the selection of impurities are provided in *A3.1.1 Hydrogen and Air Impurities Definition* report.

[1] https://whoairquality.shinyapps.io/AirQualityStandards/

2 Experimental Approach & Preparatory Work (A3.1)

In this section, the selection and preparation of impurities for the hydrogen contaminant mixture and air contaminant mixture is discussed (A3.1.1 and A3.1.4). Descriptions of the single cell PEMFC (A3.1.2) and short-stack PEMFC (A3.1.3) hardware are also provided.

2.1 Hydrogen contaminant mixture (A3.1.4)

Several contaminants listed in the ISO 14687:2019(D) standard were selected on the basis of their individual impact on fuel cells. A secondary consideration was the potential interaction of components if mixed. For example, ammonia, formaldehyde, and formic acid would react with each other in a mixture so the latter two were excluded despite studies showing an impact of formic acid on fuel cell performance [1]. Table 2 lists the hydrogen contaminants prepared within the mixture and respective concentrations, besides the measured compositions used at NPL and supplied to CEA. It was also necessary to define specific compounds to represent classes of impurity specified in the standard for example, non-methane hydrocarbons and total sulphur. The cylinders were prepared with concentrations 100× higher than the threshold values with the cylinders being diluted with pure hydrogen at the point of use enabling different concentrations to be supplied to the cell. A baseline mixture of 0.8 µmol mol^{-1} CO in H_2 was also prepared for baseline experiments.

Table 2 - Hydrogen contaminant mixture created on the basis of ISO 14687:2019(D) thresholds used at CEA and NPL

Components	Chemical formula	Mixture specified (µmol mol^{-1})	Mixture sent to CEA (µmol mol^{-1})	Mixture used at NPL (µmol mol^{-1})
Hydrogen	H_2		(Matrix)	
Methane	CH_4	10000	9700	10000
Toluene	C_7H_8	29	27	31
Carbon monoxide (with ^{13}C)	^{13}CO	20	23	20
Carbon monoxide (with ^{12}C)	^{12}CO		0.24	0.20
Ammonia	NH_3	10	9.5	9.8
Dichloromethane	CH_2Cl_2	2.5	2.4	2.6
Hydrogen sulphide	H_2S	0.4	0.38	0.34

2.2 Air contaminant mixture (A3.1.4)

In an internal report, *A3.1.1 Hydrogen and Air Impurities Definition* (as already reported in the 1st Interim Technical Report delivered in month (M) 09 to MSU) it was stated that two major sources of pollutants exist: exogenous (e.g. from air impurities) and endogenous (e.g., degradation of fuel cell components). A literature search was undergone to identify major pollutants of each source and it was decided in a Consortium meeting that the degradation compounds that might exit from the cells due to the degradation of the polymer membranes should not be studied in Mefhysto. Major reasons were that their analysis would require some advanced analytical techniques and resources that had not been budgeted nor allocated in the project. On the contrary, it was decided that halogenated compounds (in particular, fluorinated ones) would be evaluated in air supplies to the fuel cells. This was accomplished in the SENEPY platform, at CEA and it is a main topic in **Deliverable D5**. In this second deliverable of WP3,

a protocol developed by UDC, with the collaboration of NPL and CEA, to sample air and hydrogen is defined and validated to analyze halogenated volatile compounds (in particular, fluorinated ones). Also, an analytical methodology was implemented to quantify them, details can be found in **Deliverable D5**.

Several atmospheric contaminants were identified from literature [2]–[5] and chosen based on anticipated impact on PEMFC (Table 3). At NPL a cylinder was prepared with the components indicated below. It was anticipated that some reaction between the impurities and the matrix gasses may occur however was not possible to quantify the stability of the air mixture used so the concentrations indicated below are for guidance only and are not traceable. At CEA, it was decided that components in Table 3 should be mixed at the point of use so no air impurity cylinders were delivered to CEA.

Table 3 - Air contaminant mixture prepared and used at NPL, representing major atmospheric contaminants and concentrations measured in the UK and EU

Components	Chemical formula	Mixture specified (µmol mol^{-1})	Mixture used at NPL (µmol mol^{-1})
Nitrogen	N_2	(Matrix)	
Nitrous oxide	NO	5	5.326
Ammonia	NH_3	5	4.968
Toluene	C_7H_8	0.25	0.242
Sulphur dioxide	SO_2	2.5	2.576

As with the hydrogen cylinder this air contaminant mixture was diluted with compressed air at the point of use. For drive cycle (Fuel Cell – Dynamic Load Cycling, or FC-DLC) testing the air contaminant mixtures were diluted to three concentration ranges, representing low, medium (threshold) and high concentrations. Correspondingly, their exposure during drive cycles was varied as well, as indicated in Table 4. Note that fluorinated compounds in air were not considered because they were the object of another task (A3,4,3) to be performed in the final months of the project (in particular during M36), as scheduled.

Table 4 - Concentrations of air contaminants for testing during FC-DLC; 100 hours of FC-DLC consists of 305 repeated cycles)

Contaminants	Low range (nmol mol^{-1})	Medium range (nmol mol^{-1})	Peak value (nmol mol^{-1})
NO	100	500	1000
NH_3	100	500	1000
C_7H_8	5	25	50
SO_2	50	250	500
Exposure duration	*Constant during FC-DLC*	*3 cycles every 50 cycles*	*1 cycle every 100 cycles*

2.3 Single cell PEMFC (A3.1.2)

Single cell PEMFC hardware was defined by CEA and NPL and identical hardware was used at both organisations though with different components used. Cell endplates, current collectors and flow field plates were the same, but a different make of gas diffusion layers and catalyst coated membrane was used at NPL. The setup comprised of a 25 cm^2 active area cell, with single channel graphitic flow field plates assembled in a counter-flow configuration. The flow fields and current collectors were electrically isolated from compression plates to prevent

short circuiting the cell via the test station. At NPL copper heat exchangers were attached to the compression plates to provide a dynamic temperature control.

At CEA, Different gas combinations were tested using 4 distinct fuel cell conditions which will be referred to as Break-In condition, CEA conditions, AutoStackCore conditions (from a previous EU project) and European Harmonized conditions for automotive as defined by JRC. Single cell tests were carried out using a commercial Gore PRIMEA Catalyst Coated Membrane (CCM) (composition A 510.1/M 820.15/C 580.4) and 22BB commercial Gas Diffusion Layers (GDL). The GDL was hot-pressed onto the CCM to form the complete MEA before the assembly of the 25 cm² single cell.

The four different testing conditions are detailed in the following Table 5.

Table 5 - Summary of the 4 different operating conditions

Pol Curve	*Break-in conditions*	CEA conditions	ASC conditions	Harmonized EU automotive conditions[2]
Sto H_2/Air	1.5 / 2.0	1.5 / 2.0	1.4 / 1.8	1.3/1.5
RH Anode/Cath *(dew point °C)*	80% / 80% (74°C / 74°C)	50% / 50% (74°C / 74°C)	40% / 50% 49°C / 53°C	50%/30% (64°C / 53°C)
Pressure Anode/Cath (bar abs)	1.5/1.5	1.5/1.5	2.2 / 2.0	2.5 / 2.3
Cell Temperature	*80°C*	*80°C*	68°C	80°C
Minimum flowrate	Equivalent to 0.2 A/cm² by default value–		Increased to equivalent to 0.4 A/cm² to avoid flooding of the cell at low current density	

2.4 Short-stack PEMFC (A3.1.3)

Identical water-cooled F-design short-stack PEMFCs containing 8 cells, each cell with an active area of 220 cm² were built at CEA using MEA supplied by NPL from HyPlat (Table 6). Identical electrodes were also used for NPL's single cell testing.

This F-design has been conceived at CEA using serpentine designs at the anode and cathode circuits. After stack assembly, an initial break-in step has been performed for several hours at CEA to reach the nominal performances of the stack before any further characterizations. The break-in conditions are summarized in Table 5 (similar both in single cell and F-stack). A polarization curve in CEA reference conditions (see Table 5) is then performed according to the STACKTEST[3] procedures to validate the performance level at beginning of life.
After break-in, the performances of both stack are similar and are thus comparable.

[2] Tsotridis G, et al. EU HARMONISED TEST PROTOCOLS FOR PEMFC MEA TESTING IN SINGLE CELL CONFIGURATION FOR AUTOMOTIVE APPLICATIONS. EUR 27632. Luxembourg (Luxembourg): Publications Office of the European Union; 2015. JRC99115

[3] http://stacktest.zsw-bw.de/fileadmin/stacktest/docs/Information_Material/Performance/TMs/TM_P-08_Polarisation_Curve.pdf

3 Experimental

3.1 NPL Short-Stack[4] Experimental

3.1.1 Materials

An 8-cell short-stack PEMFC was assembled by CEA using MEAs from HyPlat (South Africa) with specifications shown in Table 6 and supplied to NPL.

Table 6 - Specification of MEAs from HyPlat (South Africa)

Component	Description
Membrane	**Goreselect™ M735.18 – 18 µm chemically and mechanically durable membrane suitable for high power density applications**
Catalyst layer	**Pt/C – corrosion resistant carbon, load cycling resistant electrocatalyst at 0.1 mg_{Pt} cm^{-2} (anode) and 0.4 mg_{Pt} cm^{-2} (cathode)**
Sub-gasket	**PET 80 ± 5 µm**
Gas diffusion layer	**Freudenberg H14CX483 – c.a. 186 µm thickness with hydrophobic treatment and microporous layer**

ASTM Type 1 deionised water (Elga Purelab) was used throughout. Pure hydrogen was supplied by a hydrogen generator (Hogen S-Series 2) with a nominal purity of 99.9995 % (<5 µmol mol^{-1} water, <2 µmol mol^{-1} nitrogen, <1 µmol mol^{-1} oxygen). Compressed, dry air compliant with ISO 8573-1 class 1.2.1 was used for the cathode supply. Nitrogen used for purging was produced by a generator (Apex GasGen Nevis) with nominal purity of 99.9995 % (5 µmol mol^{-1} residual oxygen). Reference CO measurements were performed using a cylinder containing 79.3 µmol mol^{-1} CO and 5.06 µmol mol^{-1} CH_4 in a matrix of hydrogen diluted to the required concentration accordingly.

3.1.2 Equipment

Short-stack testing was performed on a fully automated fuel cell test station (G100, Greenlight Innovation, CA). T-type thermocouples were embedded in the gas inlets as well as the inlet/outlet of the water jacket. Further specifications for the stack are given in Table 7. Nominal current density for the stack was set based on the corresponding voltage (0.65 – 0.7 V) at the given current density.

Table 7 – Specifications of CEA stack

Specification	Units	CEA stack
Active area	cm^2	220
Number of cells	-	8
Nominal operating current density	A cm^{-2}	0.7 (range 0.5 to 1 A/cm^2)
Cooling method	-	Water jacket

A dilution system was built to facilitate gas mixing into the anode. The system comprised of two low flowrate hydrogen flow meter/controllers (Bronkhorst EL-FLOW® Select, max flow 300 mL min^{-1}) and one high flowrate flow meter/controller (Bronkhorst EL-FLOW® Select, max flow 30 L min^{-1}) that diluted the contaminants with pure hydrogen. FlowView™ software (ver. 1.23) was used to dynamically control the flows in a master (pure hydrogen) and slave (contaminants) configuration.

[4] Chapter 9 – Fuel Cell short stack testing, *Fuel Cells for Transportation – Fundamental Principles and Applications*, 2023, 253-278

3.1.3 Methods

The parameters shown in Table 8 were used for operation. Anode humidification was by-passed at NPL to ensure that water soluble impurities were not lost in the humidification systems. This was compensated for with a higher relative humidity on the cathode. Anode and cathode pressures were also controlled at the outlet. These parameters were used upon start-up and remained unchanged throughout short-stack testing.

Table 8 - Short-stack operating conditions used in CEA and NPL

	Parameter	Units	CEA conditions	NPL conditions
	Coolant inlet temperature	°C	80	80
Anode	Anode operating pressure	kPag	50	50
	Anode inlet temperature	°C	90	90
	Anode stoichiometry (H_2)	-	1.5	1.5
	Anode humidity (dewpoint temperature)	% RH (°C)	50% (64)(but no direct humidification in recirculation mode)	-
Cathode	Cathode inlet temperature	°C	90	90
	Cathode operating pressure	kPag	50	50
	Cathode stoichiometry (air)	-	2	2
	Cathode humidity (dewpoint temperature)	% RH (°C)	50% (64)	80% (74)
	Minimum current density for stoichiometry operation	A cm^{-2}	0.2	0.3

The short-stack was first tested with CO/H_2 mixtures at 0.2 µmol mol^{-1} and 0.8 µmol mol^{-1} to develop a baseline understanding of their tolerance to poisoning and recoverability afterwards. A standardised procedure was implemented whereby the stacks were operated at nominal voltages with pure hydrogen to establish baseline performance before being poisoned for up to 4 h. During shutdown between each test, the anode was purged with air for up to 1 h to oxidise any adsorbed CO.

Once the reference poisoning profiles had been established with CO/H_2, the same procedure was adopted for the hydrogen contaminant mixture. The mixture concentration was set to supply the equivalent of 0.2 µmol mol^{-1} and 0.8 µmol mol^{-1} of CO.

At NPL Short-stack tests were repeated using the same materials, with an overnight shutdown and air purge on the anode used to regenerate the catalyst layer in between repeats.

3.2 CEA Short-Stack Experimental

3.2.1 Materials

Same 8-cell short-stack PEMFC assembled by CEA using MEAs from HyPlat (South Africa) with specifications shown in Table 6.

The stack tested at CEA is equipped with a segmented device (S++®) between the cells 4 and 5 to record (when possible during experiments) the distribution of local current densities and temperature. The CDD mapping aims at getting additional information about impact of impurities.

Fluids used for the tests are provided by CEA premises, with deionised water as cooling medium, compressed dry filtered air for the cathode supply, pure Nitrogen from tanks for purges, safety, valves control, or electrochemical measurements, and Hydrogen 4.5 from B50 tanks, that could be analysed to confirm at least CO, CO_2, CH_4 and H_2S concentrations fulfilling the requirements of 5.0 purity level. CO used for tolerance reference measurements or impact of impurity were performed using B50 tanks containing 5 ppm CO or 0.8 ppm CO in a matrix of hydrogen, directly provided to the fuel line without dilution, shifting from pure H_2 to CO-H_2 mixture when needed during the experiments. Avoiding the dilution allowed to operate with the actual flow rate whatever the operating conditions and current applied, including no risks of differences in feeding conditions when recirculation / purges mode is used as selected for these tests (following procedures and recommendations of the projects Hydraite and MetroHyve2).

3.2.2 Equipment

Short-stack testing was performed on a CEA-home-made automated fuel cell test station for few cells short stacks and about 1kW electric power maximum.

The test station (see Figure 2) is adapted to operate flow-through mode, dead-end or recirculation + dead-end with purges; this last mode was selected for this project.

In addition, gas analysers to check composition in CO, CO_2, CH_4, O_2, H_2S and N_2 are available on-line with sampling performed in the recirculation loop. Impact of sampling could be studied in the project MetroHyve2.

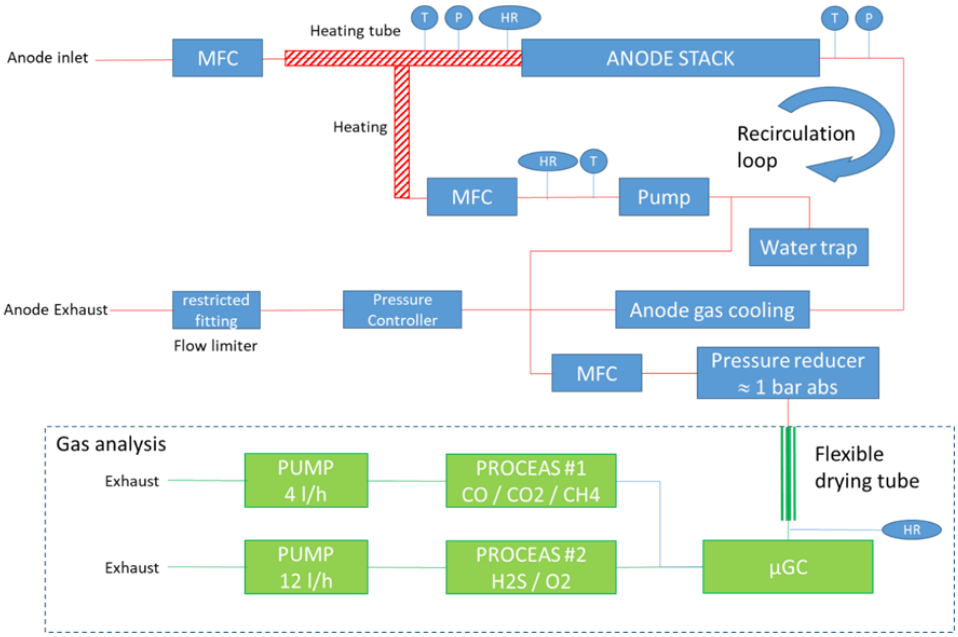

Figure 1 - Anode line on CEA short-stack test bench OBIOU

Figure 2 - CEA short-stack test bench OBIOU (left) coupled with online gas analysis for CO/CO_2 measurements (Proceas equipment) with H_2 recirculation loop (right)

For the tests presented here, the set of operating conditions was selected for both the fuel feeding conditions and gas sampling/analyses, based on MetroHyve2 outcomes.
Specifications for the stack are given in Table 7. Nominal current density for the stack was set based on the corresponding voltage (0.65 – 0.7 V) at the given current density. Tests have been conducted in the nominal conditions and in conditions with a temperature reduced by 10 °C to enhance the impact of impurity and get more significant data with 0.8 ppm CO. These conditions have been applied at fixed loads of 0.6 and 1.0 A/cm² and one test was conducted during about 100 hours of FC-DLC.

3.2.3 Initial performances of short-stacks

As previously mentioned, two identical short-stacks were prepared at CEA. After the initial break-in phase, they were characterized in performances under CEA reference conditions (see Table 5) and the results are presented in Figure 3. Both stacks show very close performances (only 10 mV gap at 1 A/cm²) which guarantees the possible comparison between NPL and CEA experiments. Moreover, NPL also compared these performances obtained on CEA lab test bench with the performances measured on their test bench (see section 4.3 and Figure 18).

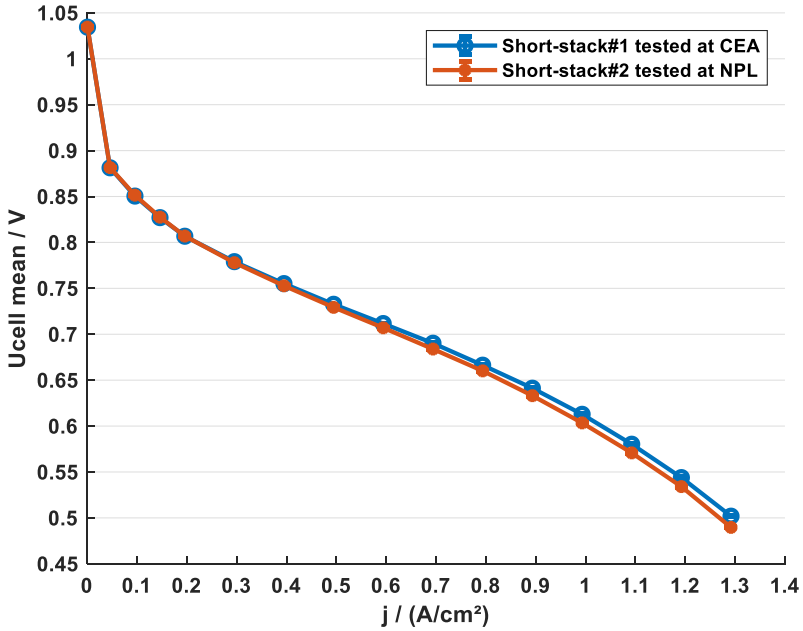

Figure 3 - Initial polarization curves under CEA reference conditions for both F-designed short-stacks

3.2.4 Methods

The parameters shown in Table 8 were used for operation at least for the nominal case. Anode humidification was bypassed for the operation on recirculation mode with purges. The selected sets of conditions for the Hydrogen were a recirculation flow rate of 10Nl/min, and purges of 0.5s each 60s. The nominal conditions were applied with 1.5 bars for both fuel and air inlet pressures, and 50 % relative humidity for air. These parameters remained unchanged throughout short-stack testing. One parameter was changed: the stack inlet temperature was set at 80 °C as it is specified for stack-F nominal conditions, but some experiments were conducted at 70 °C to decrease somehow the tolerance and get more significant impact on cells voltage when polluting the stack with 0.8 ppm CO in H_2 mixtures.

Tests have been performed at fixed current densities of 0.6 or 1 A/cm² or following the FC-DLC load profile with a maximum current density of 1.2 A/cm².

Following outcomes of the projects Hydraite and more recently of the project MetroHyve2, most appropriate operation mode and protocols have been selected and applied to this stack made for Mefhysto. Below are listed the different types of experiments conducted:

- Reference tests including
  - polarisation curve recorded under pure Hydrogen (without impurities) to check performance
  - and tolerance test to 5 ppm CO (tolerance is assessed checking the voltage decrease after shifting from pure H_2 to mixture H_2 + 5 ppm CO) during about 1 hour or until more than 50 mV loss (when possible to stop in time because after 50 mV loss, the decrease can be quick and reach more than 100 mV before shifting back to pure H_2).
- Electrochemical characterization of electrodes at beginning of life (or beginning of test), then to be repeated at end of test to check possible degradations: cyclic voltammetry applied on cathodes and anodes of the stack.
- Poisoning tests (impact of impurity) during few hours to be consistent with a daily operation of a vehicle with a selected concentration of 0.8 ppm CO in Hydrogen:
  - At fixed current density of 0.6 A/cm² (average voltage about 0.72V)
  - At fixed current density of 1 A/cm² (average voltage about 0.69V)

- During FC-DLC (applied with a maximum current density of 1.2 A/cm²)

First plan was to conduct these poisoning tests in the nominal operating conditions corresponding to the selected design; however because these conditions include operation at 80 °C, which is known to increasing notably the tolerance, tests have been conducted also at 70 °C to get a more significant information, at least for operation

- Tolerance tests to check the impact of shut-down procedure after poisoning applied during stack tests to ensure better measurements and viable information on the impact of impurities: following outcomes of Metrohyve2, these experiments have been done to check how the tolerance to 5 ppm CO is affected after:
  - Tolerance test + shut-down with air cleaning
  - Tolerance test + shut-down without air cleaning
- With different cases for the history before the first tolerance test, the sequence of a daily test was the following: start-up, stabilization at fixed current density under pure H_2, 5 ppm CO 1st tolerance test (~1 hour or less if voltage loss is more than 50 mV), back to pure H_2 for at least 10 minutes, shut-down protocol and one repetition for the 2nd tolerance test of the day.
- Impact of a short ageing period of 100 hours of load cycles on the tolerance to CO: the sequence of test was the following: start-up, stabilization at fixed current density , launching of FC-DLC under pure H_2 for 100 h, back to fixed current density, stabilization at fixed i, application of the 5 ppm CO 1st tolerance test (~1 hour or less if voltage loss is more than 50 mV), back to pure H_2 for 10 minutes, shut-down with air cleaning and repetition with a 2nd tolerance test. The 2 tolerance tests are aiming at checking reversible or non-reversible impact of the load cycles on the tolerance.

3.3 NPL Single Cell Experimental

3.3.1 Materials

Catalyst coated membranes (CCMs) were obtained from HyPlat (South Africa). The membrane and catalyst layer specifications are similar to that in Table 6 that were used for short-stack testing. Freudenberg H23C6. The CCM and GDLs were not hot-pressed, rather just overlayed carefully during assembly. Silicone gaskets (250 µm thickness) on either side of the CCM provided sealing.

ASTM Type 1 deionised water (Elga Purelab) was used throughout. Pure hydrogen was supplied by a hydrogen generator (Hogen S-Series 2) with a nominal purity of 99.9995 %. Compressed, dry air compliant with ISO 8573-1 class 1.2.1 was used for the cathode supply. Nitrogen used for purging was produced by a generator (Apex GasGen Nevis) with nominal purity of 99.9995 %.

3.3.2 Equipment

Single cell testing was performed in a fully automated fuel cell test station (G60, Greenlight Innovation, CA) coupled with a potentiostat/galvanostat/frequency response analyser (Gamry Reference 3000). Temperature monitoring and control was realised using T-type thermocouples embedded on the gas inlets/outlets, in the anode/cathode flow field plates and at the inlet/outlet of the miniature heat exchanger on the cell.

Dilution of contaminants for testing was carried out using hydrogen flow meter/controllers (Bronkhorst EL-FLOW® Select, max flow 300 mL min^{-1}) for the anode. On the cathode, air contaminants were diluted using an air mass flow controller (Brooks, 5850 E Series, max flow 1 L min^{-1}) connected to an external control unit (Brooks 0154).

3.3.3 Methods

3.3.3.1 Dosage response

The first test performed on the single cell PEMFC was the dosage response test with contaminant mixtures. For hydrogen contaminants, this was achieved by blending the hydrogen contaminant mixture at 1 %, 2 % and 5 % into pure hydrogen. For air impurities, the low range concentration specified in Table 4 was achieved using a 2 % blend of the prepared contaminant cylinder in compressed air.

Tests were carried out by first measuring the baseline galvanostatic performance of the cell at 1 A cm^{-2} with pure gases and then supplying the contaminated mixtures for 2 – 3 h. In the case of the hydrogen contaminant mixture, the concentration was sequentially increased from 1 % to 5 % with a 1 h recovery period in between where pure gases were restored. Operating parameters for the dosage response test and FC-DLC are shown in Table 9.

Table 9 - Operating parameters used for single cell PEMFC testing

	Parameter	Units	Start-up & Break in	Characterisation & Testing
	Operating temperature	°C	80	80
Anode	Anode operating pressure	kPag	150	150
	Anode inlet temperature	°C	90	90
	Anode stoichiometry (H_2)	-	1.5	2
	Anode humidity (dewpoint temperature)	% RH (°C)	80 % (74)	50 % (64)
Cathode	Cathode inlet temperature	°C	90	90
	Cathode operating pressure	kPag	150	150
	Cathode stoichiometry (air)	-	2	2
	Cathode humidity (dewpoint temperature)	% RH (°C)	80 % (74)	50 % (64)
	Minimum current density for stoichiometry operation	A cm^{-2}	0.2	0.2

3.3.3.2 FC-DLC

The single cell operating conditions for start-up, break in, characterisation and testing are shown in Table 9.

Anode and cathode pressures were also set to 150 kPag and controlled at the gas outlets.

FC-DLC testing was performed in the steps shown in Figure 4. The test was performed in 100 h increments, allowing for characterisation and shutdown for recovery in between every 100 h.

Nominal operating current density for the single cell was 1 A cm^{-2} corresponding to 0.65 V - 0.7 V while the stack load values during FC-DLC were set based on the percentage

of the max current, defined at 0.6 V on the polarisation curve recorded during baseline characterisation. The FC-DLC parameters were adapted from the EU Harmonised Single Cell PEMFC Testing Protocols [6], and are based on repeated urban and extra-urban drive cycles.

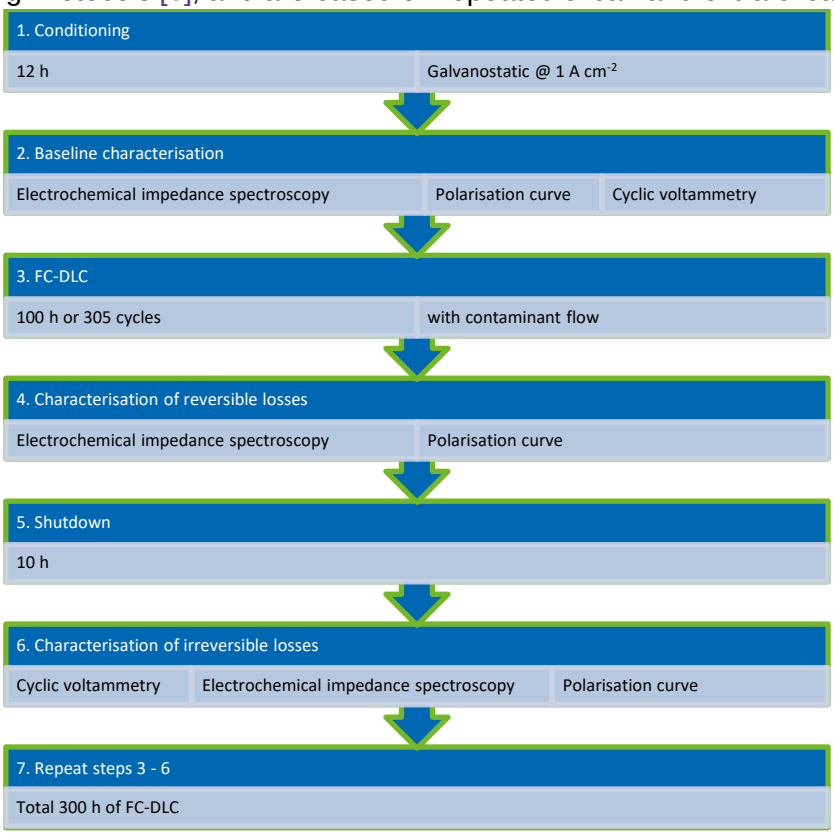

Figure 4 - Procedure used for single cell FC-DLC testing with contaminant mixtures

3.4 Proton Pump

For Task A3.2.1, it was determined that a proton pump cell running with high stoichiometry (equivalent to a differential cell) and a dry impure hydrogen supply would be the most valuable technique for NPL to study the correlation between electrochemical measurements (polarisation curves and impedance spectroscopy) with contamination processes when a combination of contaminants is present. Other experiments, such as rotating disk electrode (RDE) experiments are ex situ methods to evaluate catalyst performance and do not provide tests at relevant concentrations and issues with the solubility of some impurities in the complex mixtures chosen for study would make measurements imprecise. Contemporary work by NPL funded through another project, developed this a proton pump cell and make it available for these measurements. Further work by NPL in the area [7] besides work performed in MefHySto WP1, and MetroHyVe2 showed that the impurity concentrations being studied would be below the limit of detection of a microGC (ca. 10 µmol mol^{-1}) so online gas analysis was performed by NPL on these proton pumps where relevant concentrations would be < 1 µmol mol^{-1}.

In a proton pump hydrogen oxidation occurs at the anode and hydrogen evolution occurs at the cathode, driven by a voltage between the electrodes. As the hydrogen oxidation reaction is the same as that occurring at the anode of a fuel cell but the cathode reaction is much more stable and no oxygen is present to mitigate poisoning these cells are ideal model systems for studying the impact of impurities on fuel cell anodes.

3.4.1 Materials

CCMs were obtained from FuelCellStore, utilising a PFSA D15-R ePTFE reinforced proton exchange membrane. Anode catalyst was 20 wt.% PtNi/C while the cathode catalyst was 40 wt.% Pt/C. Geometric loadings were 0.08 mg_{Pt} cm^{-2} and 0.3 mg_{Pt} cm^{-2} for the anode and cathode respectively. Gas diffusion layers with hydrophobic treated microporous layer (Freudenberg H23C6, FuelCellStore, USA) were used. For cell sealing and compression, Freudenberg HRG Ice Cube gaskets were used; P78 (0.03 mm) at the anode and P88 (0.08 mm) at the cathode respectively.

ASTM Type 1 deionised water (Elga Purelab) was used throughout. Pure hydrogen was supplied by a hydrogen generator (Hogen S-Series 2) with a nominal purity of 99.9995 %. Reference CO measurements were performed using a cylinder containing 9.74 µmol mol^{-1} CO in a matrix of hydrogen diluted to the required concentration accordingly.

3.4.2 Equipment

The proton pump cell was designed in-house with a 4 cm^2 active area with differing flow fields on either electrode. The anode flow field featured 9 parallel flow channels with 1 mm land and channel widths while the cathode flow field featured a 4-channel serpentine design.

Electrochemical measurements were made using a multi-channel potentiostat (Ivium-n-Stat) and cooling (or heating) water was supplied using a Julabo recirculating bath. Heat was supplied via a shell-tube heat exchanger with the water supplied to the proton pump in a closed loop as it was also used to humidify the cell. A schematic of the proton pump setup including peripheral equipment is shown in Figure 5.

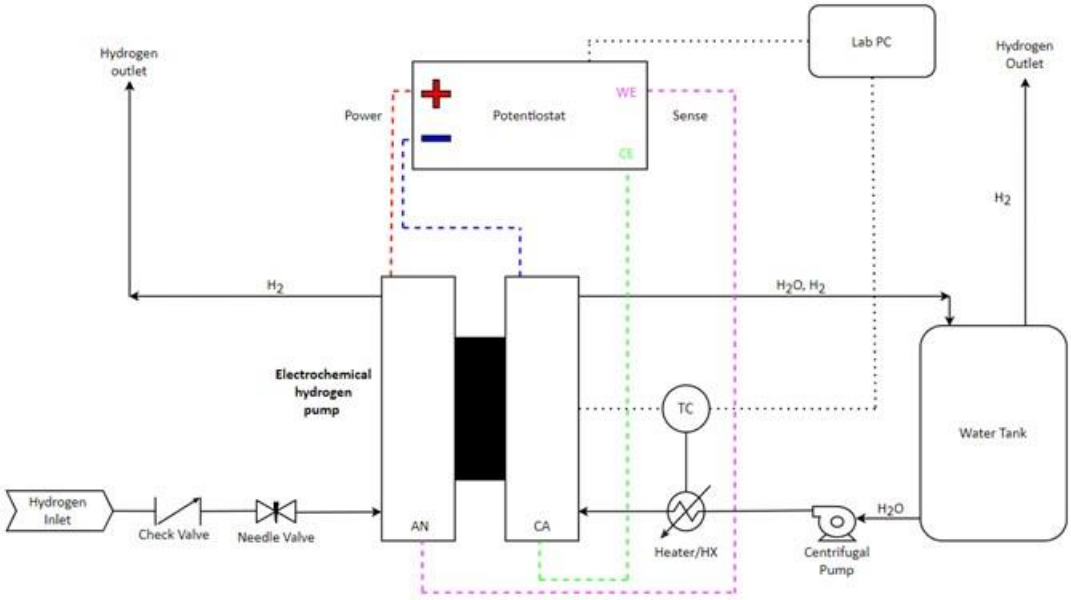

Figure 5 - Schematic of proton pump setup

A dilution system was built to supply accurate concentrations of the hydrogen contaminant mixture on a volumetric flowrate basis. The system consisted of two Bronkhorst hydrogen flow meter/controllers (EL-FLOW Select, max flow 300 mL min^{-1}) that diluted the contaminant mixture with pure hydrogen, using FlowView™ software (ver. 1.23). Flowrate into the cell was controlled at 100 mL min^{-1} using a MASS-VIEW® flow meter (max flow 200 mL min^{-1}).

3.4.3 Methods

The cell was operated nominally at 250 mA cm^{-2} and at 40 °C. The testing protocol used follows the steps shown in Figure 6 where the performance of the proton pump was measured using chronopotentiometry for 24 h before, during, and after poisoning. The cell was further characterised using electrochemical impedance spectroscopy and polarisation curve measurements immediately after the chronopotentiometry phases. At the beginning of testing, alternating steps of open circuit and chronopotentiometry were used to evaluate the stability of the proton pump during start-up/shutdown cycles.

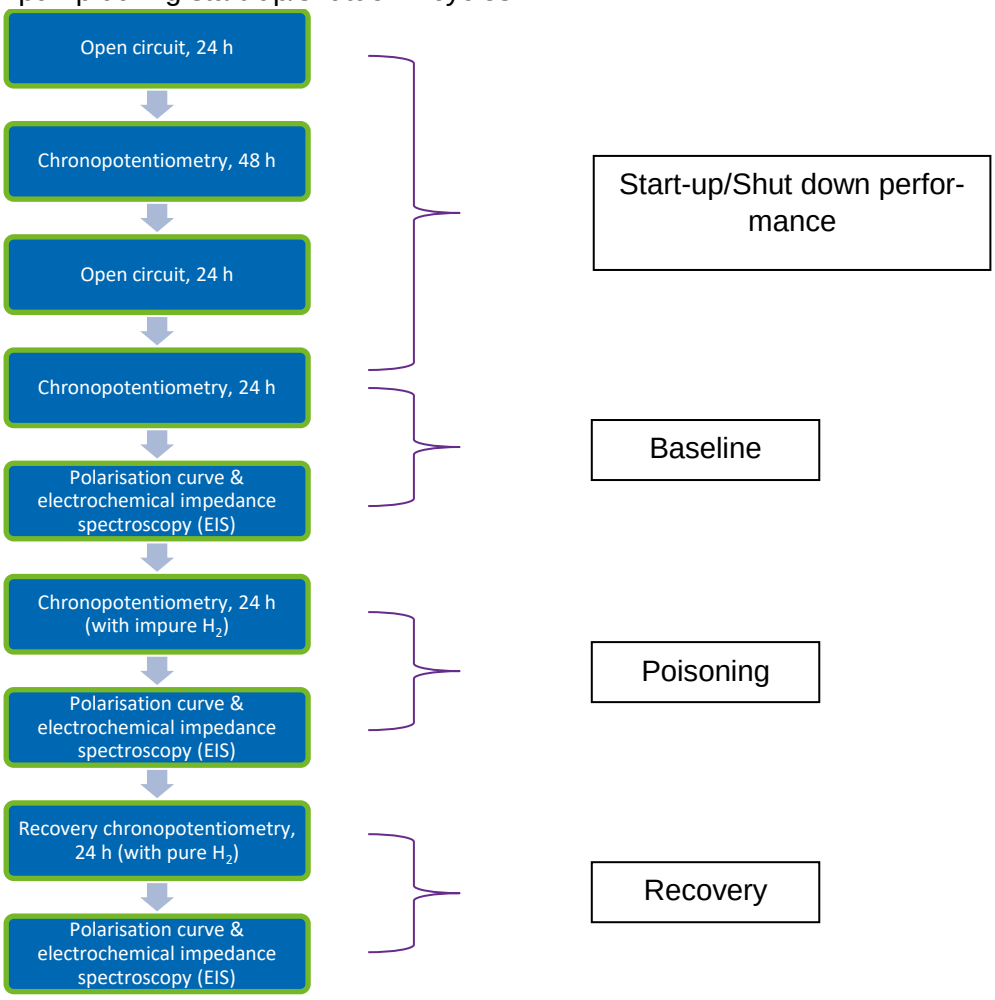

Figure 6 - Proton pump testing procedure

At NPL single cell tests were repeated with fresh materials (catalyst coated membranes, gas diffusion layers) and reassembled for each repetition, likewise for proton pump tests.

3.5 CEA Single Cell Experimental

3.5.1 General experimental procedures

The bench start-up procedure is described below:

- Supply N_2/N_2
- Turn on Pressure control and cell/bubbler heating (+ pre-heat the inlet gas pipes to T_{cell} +10 °C)
- Wait for 15 min
- Close N_2 valve at anode side, supply H_2 for 2 min @ 500 NmL/min
- Close N_2 valve at cathode side, supply Air (or N_2 + O_2 mixture) @ 1000 NmL min^{-1} for 1 min
- Connect and Start load (set minimum voltage threshold to 0,4 V)
- Increase current from 0 to 10 A with 1 min steps
- Wait for 2 min
- Turn on reactant stoichiometries above 10 A
- Wait for 2 min
- Progressive increase current from with 1 A steps until 25 A is reached or U < 0.5 V

The bench shut-down procedure is described below:

- Decrease current to 0 stepwise and disconnect the load
- Close Air valve, supply N_2 at the cathode
- Decrease Gas Pressures to Patm on both sides
- Purge air at the cathode with N_2 for 10 min
- Close H_2 valve, supply N_2 at the anode side
- Purge anode + cathode for 10 more min
- Turn off and by-pass bubblers
- Dry N_2/N_2 supply for 5 min (liquid water exhaust)
- Turn off cell heating
- Wait for 5 minutes
- Stop N_2 supply

Both start-up and shut-down protocols enable to avoid degrading conditions related to the generation of an H_2|air front at the anode which could strongly damage the MEA.

Polarization curve measurements are performed according to the STACKTEST procedures and JRC Harmonized protocol. First, conditioning step is applied to ensure stationary conditions within the cell. Then, increasing current steps until Ucell gets below 0.5 V are applied Performance are then measured during the decreasing current steps. The entire protocol is described in and illustrated in Table 10.

Table 10 – Detailed polarization curve protocol used in single cell at CEA

Step	Current density	Dwell time
Conditioning	1 A/cm²	30 min
Current increase	+ 0.2 A/cm² Until U cell < 0.5 V	1 min
Current decrease (corresponding to Pol. Curve)	-0.2 A/cm² down to 0.4 A/cm²	3 min
	-0.1 A/cm² from 0.3 down to 0.1 A/cm²	2 min
	0.05 A/cm²	2 min
	0.025 A/cm²	2 min
	OCP	1 min
Back to initial value	*0.1 A/cm²*	*1 min*
	+0.1 A/cm² up to 0.4 A/cm²	*1min*
	+0.2 A/cm² up to 1 A/cm²	*1 min*

The composition of the Fuel Cell Dynamic Load Cycle (FC-DLC) is detailed in Table 11 and illustrated in Figure 8. This pattern is divided by a low/medium power phase representative of urban driving followed by a medium/high power phase for highway driving. In single cell experiment, the maximum current value is defined when U_{cell} reaches 0.6 V at the beginning of life. The overall aging test procedure is summarized in Figure 7.

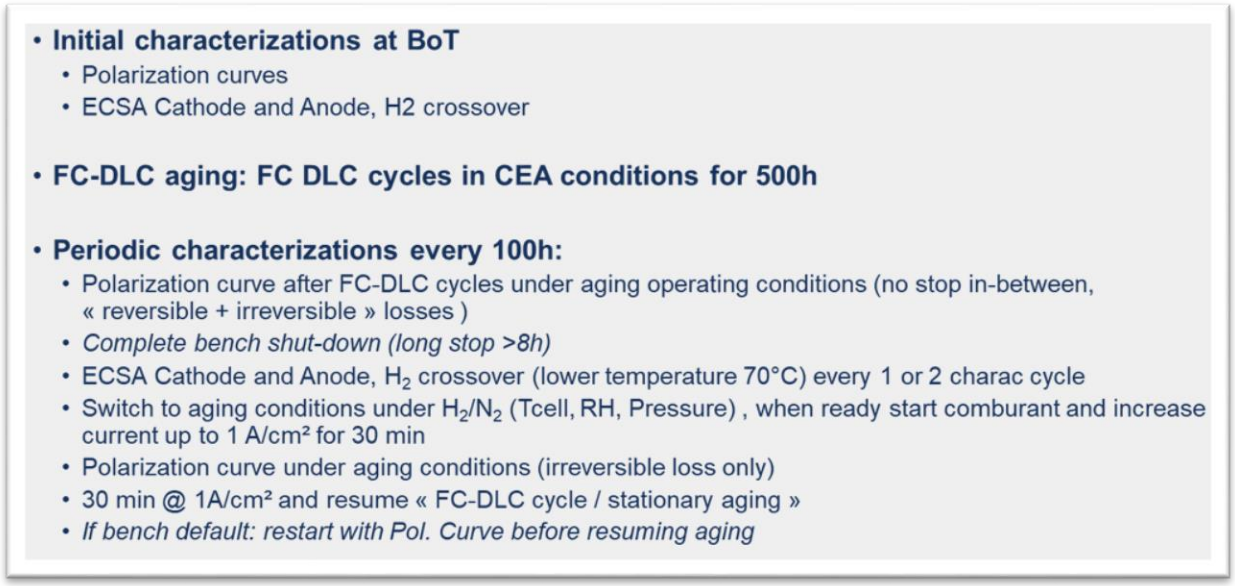

Figure 7 - Overview of aging test protocol in 25 cm² single cell

Table 11 - Detailed composition of FC-DLC cycles in term of duration and load current percentage

Step	Cumulated test time [s]	Dwell time [s]	Stack load [%]	Exemplary stack load [A]	Load steps for pseduo polarisation curve
1	15	15	0	0	
2	28	13	12.5	9.6	
3	61	33	5	3.8	
4	96	35	26.7	20.6	
5	143	47	5	3.8	
6	163	20	41.7	32.1	
7	188	25	29.2	22.5	
8	210	22	5	3.8	
9	223	13	12.5	9.6	
10	256	33	5	3.8	
11	291	35	26.7	20.6	
12	338	47	5	3.8	
13	358	20	41.7	32.1	
14	383	25	29.2	22.5	
15	405	22	5	3.8	
16	418	13	12.5	9.6	
17	451	33	5	3.8	
18	486	35	26.7	20.6	
19	533	47	5	3.8	
20	553	20	41.7	32.1	
21	578	25	29.2	22.5	
22	600	22	5	3.8	
23	613	13	12.5	9.6	x
24	646	33	5	3.8	
25	681	35	26.7	20.6	
26	728	47	5	3.8	
27	748	20	41.7	32.1	
28	773	25	29.2	22.5	x
29	841	68	5	3.8	x
30	899	58	58.3	44.9	
31	981	82	41.7	32.1	x
32	1066	85	58.3	44.9	x
33	1116	50	83.3	64.1	x
34	1160	44	100	77	x
35	1181	21	0	0	x

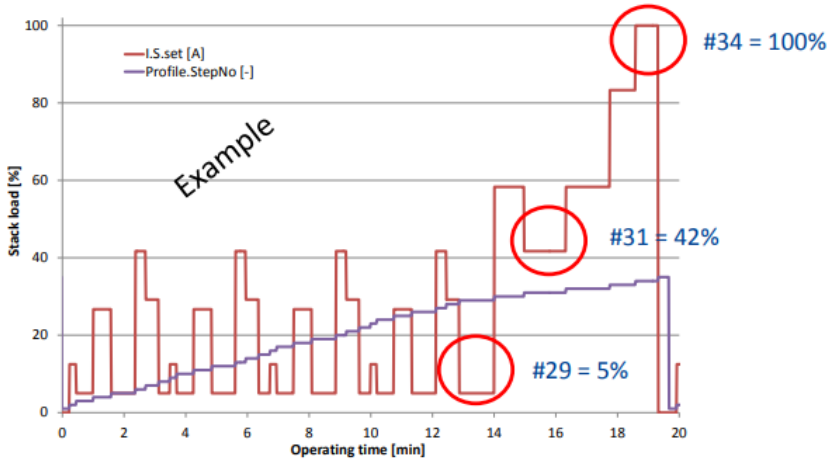

Figure 8 - Example of one FC-DLC cycle. I_{max} (100 %) is defined at 0.6 V on the BoT pol curve in CEA operating conditions

4 Results on Hydrogen contaminants (A3.2)

All relevant data recorded for this work is confidential by default in the interest of publications.

4.1 Proton Pump (A3.2.1)

Figure 9 shows an example of cell voltage evolution throughout the entire proton pump test protocol (detailed in Figure 6). The staggered baseline measured on either side of a 24 h shutdown implies good stability with an increase of < 20 mV after a shutdown-start up sequence. In contrast, the cell voltage spiked by more than 300 mV when poisoned with the hydrogen contaminant mixture. Pure hydrogen was restored during the recovery phase and cell voltage recovered to within 10 mV of the baseline value within 4 -5 h and stabilising soon after.

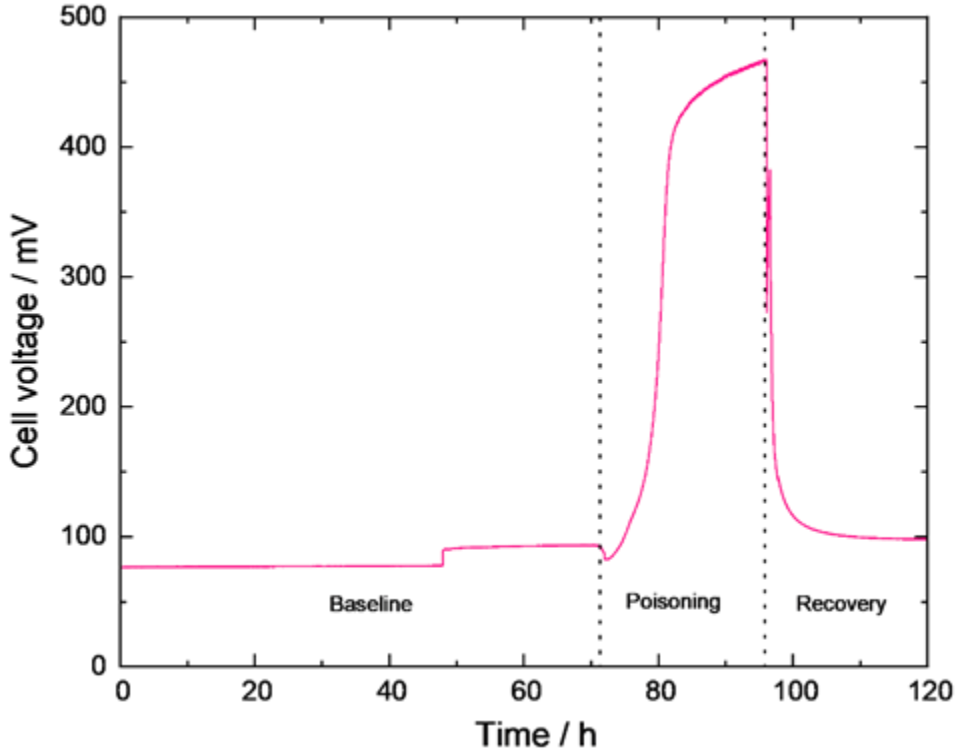

Figure 9 - Evolution of cell voltage with time through poisoning with 2 % concentration of the hydrogen contaminant mixture

The proton pump also exhibited different response times when poisoned at different concentrations of the contaminant mixture. In Figure 10, it is clearly observed that cell voltage consistently responds rapidly (50 mV increase within 6 – 10 h) with a 2 % concentration of the hydrogen contaminant mixture. Response is slower for the 1 % mixture and all 3 cells tested took more than 16 h for cell voltage to increase by 50 mV, although a higher degree of repeatability was noted in the cell response as compared to cells poisoned with 2 % of the mixture. It was also interesting to note that the reference test performed with CO and the contaminant mixture at 1 % were both supplying 0.2 µmol mol^{-1} of CO to the cell suggesting that the additional impurities do not significantly influence the cell voltage.

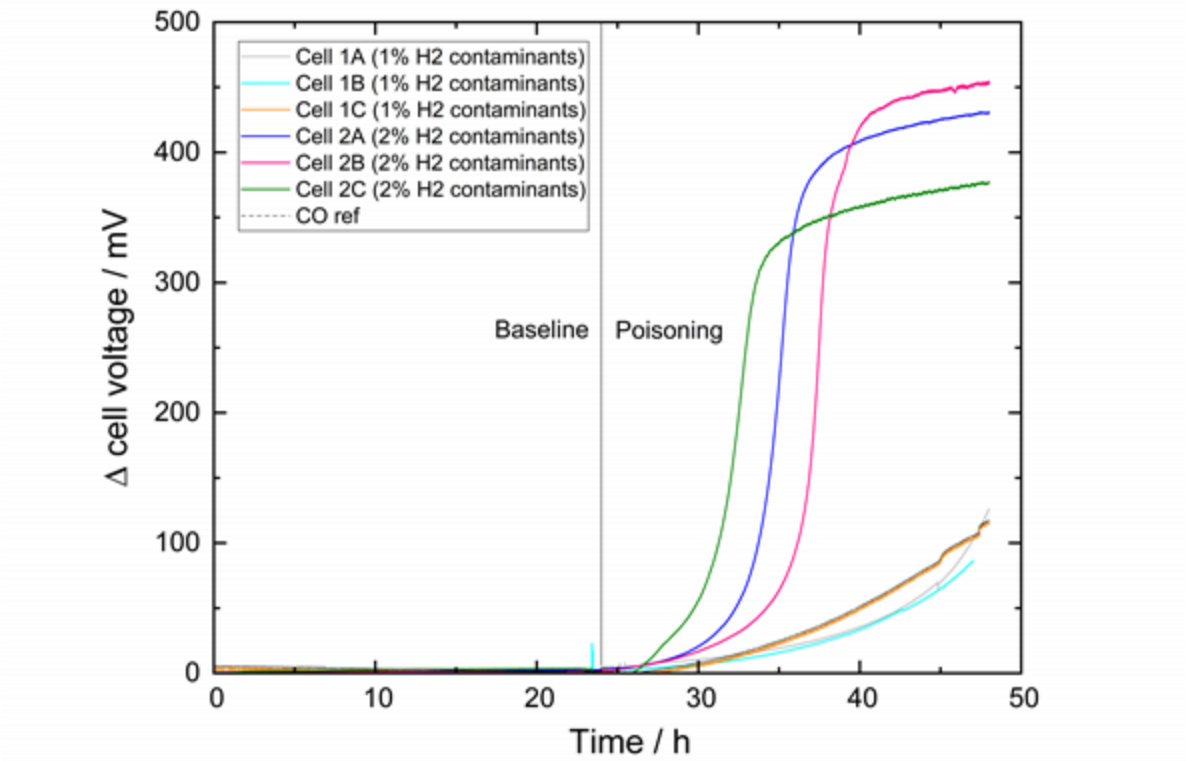

Figure 10 - Change in cell voltage over time with 1 % and 2 % concentration of the hydrogen contaminant mixture, 1 % CO as reference

Polarisation curves (Figure 11) obtained during the baseline and poisoning steps showed a clear impact of the 2 % contaminant mixture on cell performance in the intermediate to higher current densities.

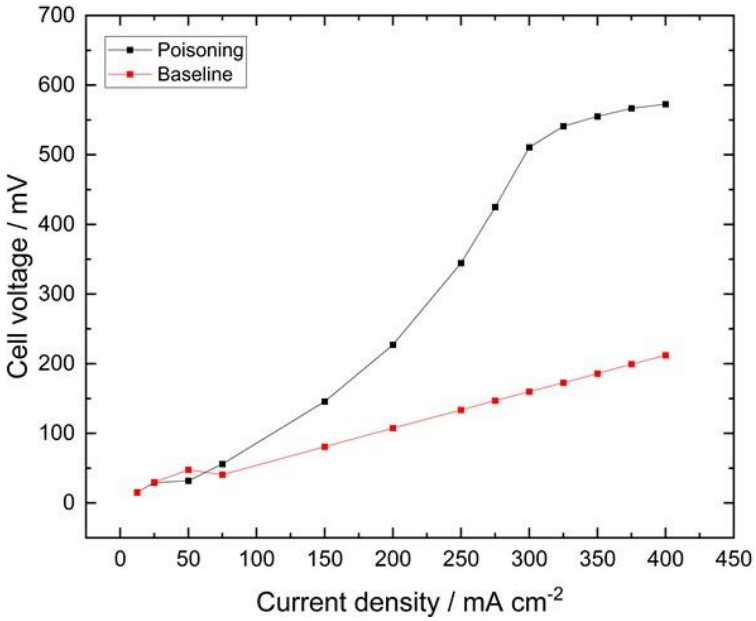

Figure 11 - Polarisation curves measured before and after poisoning with 2 % hydrogen contaminant mixture

4.2 Single Cell (A3.2.2)

4.2.1 Dosage response

Dosage response tests were performed to evaluate the impact of the hydrogen contaminant mixture on the (short-term) performance of a single cell at 3 concentrations. Tests were performed by sequentially introducing 1 %, 2 % and 5 % concentrations of the contaminant mixture, with a 1 h recovery period in pure hydrogen between each concentration increment. The corresponding voltage profiles are shown in Figure 12, along with the baseline voltage profile when pure hydrogen is supplied.

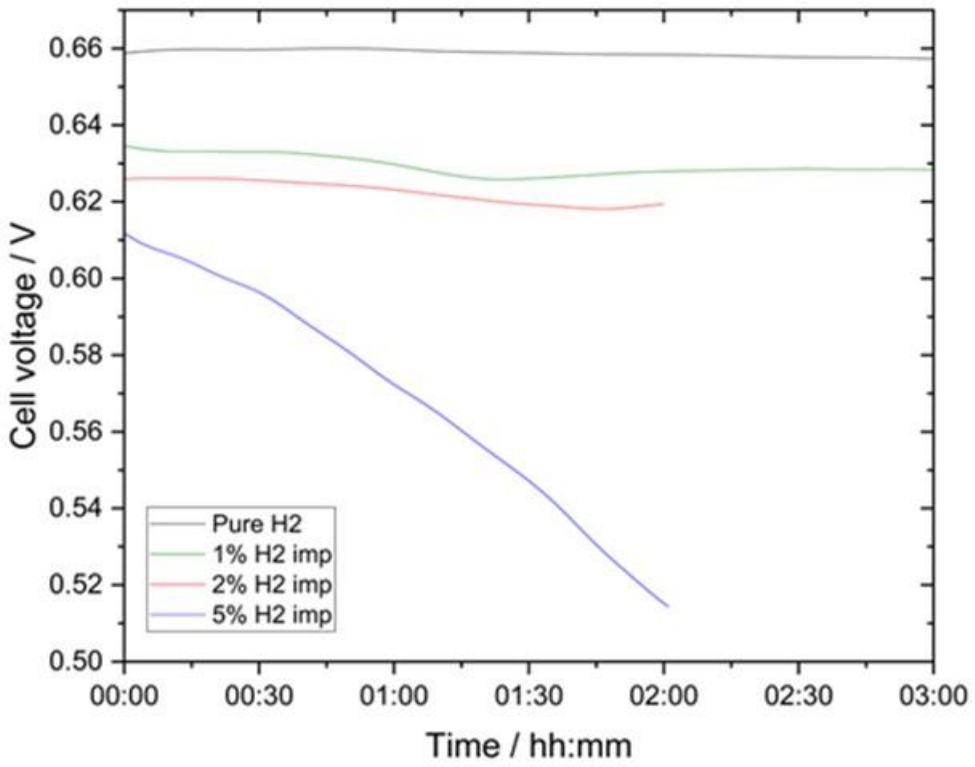

Figure 12 - Overlayed voltage decay profiles on a single cell PEMFC at different concentrations of H2 impurities

Cell voltage evolution for pure hydrogen, 1 % and 2 % contaminant concentrations are too similar to ascribe an effect caused by the contaminant. However, immediate and severe voltage decay was observed when 5 % contaminant was used.

Table 12 summarises the effects observed at the contaminant concentrations tested on 3 cells. From the voltage decays observed at the different concentrations of contaminants used, there was little separation between the baseline and 1 % contaminant post stabilisation (2 h).

Table 12: Summary of performance losses on a single cell PEMFC resulting from operating with H_2 contaminants at various concentrations

Contaminant concentrations tested	Test duration / h	Voltage decay / mV h^{-1}	Comments
Baseline (pure H_2)	3	0 – 1	-
1% H_2 contaminant mixture	3	0 – 2	Slow decay stabilising after 1.5 h
2% H_2 contaminant mixture	2	3 – 5	Slow decay stabilising after 2 h
5% H_2 contaminant mixture	2	30 – 50	Immediate decay

Polarisation curves (Figure 13) measured after each stage of poisoning showed a steep decline in cell performance after 5 % concentration of hydrogen contaminants. Cell voltage at 1 A cm^{-2} decrease by 15 mV between the baseline and 2 % concentration but dipped a further 93 mV between 2 % and 5 % concentration of hydrogen contaminants. The losses were not entirely reversible as cell voltage recovered to 0.594 V at 1 A cm^{-2} after a recovery period where pure hydrogen was restored.

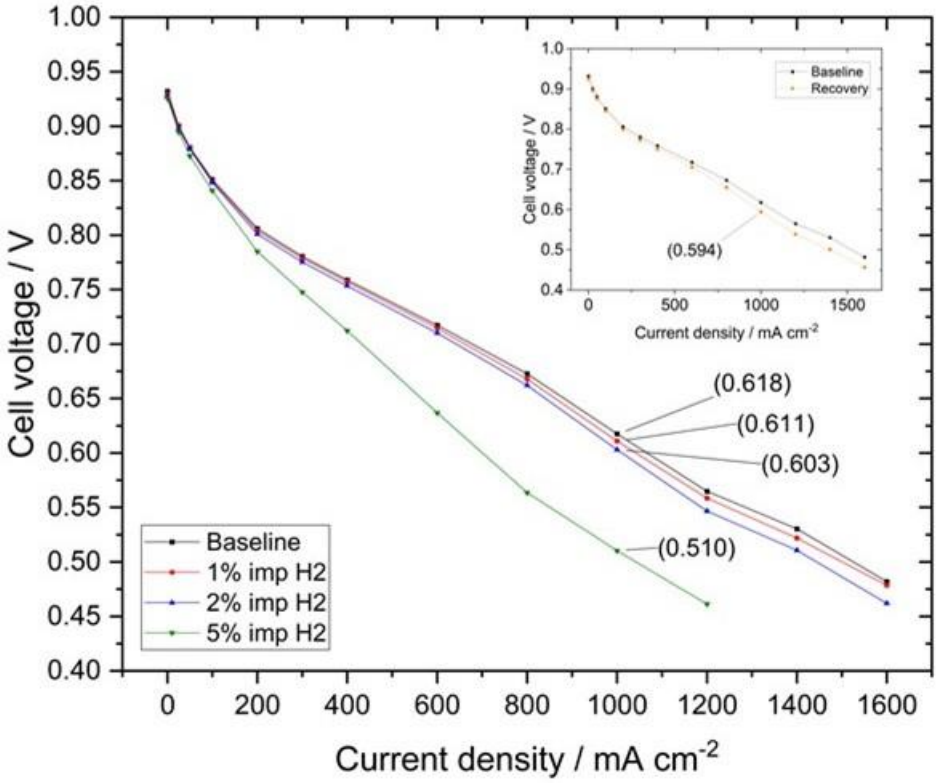

Figure 13 - Polarisation curves measured after each poisoning concentration and after recovery (inset)

Based on the results from the dosage response tests, the 2 % concentration was deemed suitable for DLC tests. The 5 % concentration deteriorated the fuel cell too quickly, while the impact of the contaminant mixture at 1 % concentration was not clearly discernible from the natural degradation of the cell.

4.2.2 Fuel Cell - Dynamic Load Cycling (DLC)

At NPL, DLC was performed for up to 300 h, using 2 % of the hydrogen contaminant mixture. Although the initial plan was to perform FC-DLC for 500 h, performance had deteriorated such that after 300 h, nominal cell voltage had dipped below 0.4 V at 1 A cm^{-2} necessitating that the cell be shut down.

Polarisation curves measured before and immediately after every 100 h of DLC show a steady decay of cell performance. From Figure 14, it is noted that voltage decay at 1 A cm^{-2} is the highest (~100 mV) between 0 and 100 h after which more steady deterioration occurs (~70 mV from 100 – 200 h and 200 – 300 h). On the reference cell fed with pure hydrogen, the voltage decay between 0 and 100 h was also the highest (~80 mV) followed by ~60 mV from 100 – 200 h. Most contrastingly, cell voltage at 1 A cm^{-2} only decreased by 19 mV between 200 h and 300 h, suggesting that 2 % concentration of the hydrogen contaminant mixture only begins to noticeably affect cell performance after >200 h of operation.

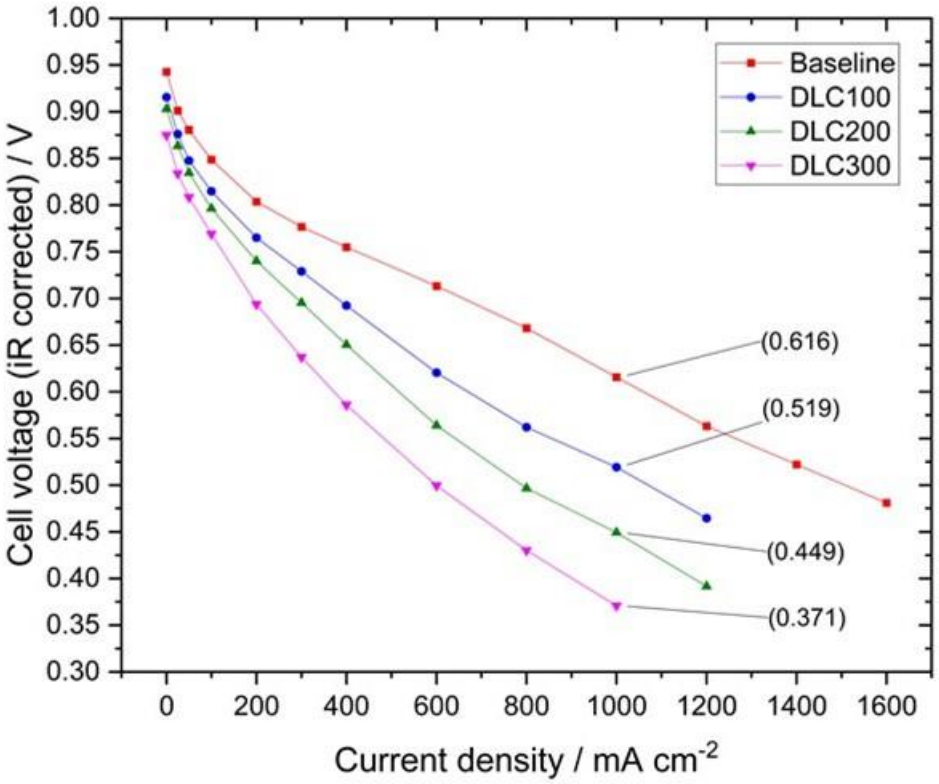

Figure 14 - Polarisation curves measured on a single cell PEMFC after every 100 h of FC-DLC

Following shutdown for 10 h, the polarisation curves measured upon restart show an improvement in cell performance. The evolution of cell voltage at open circuit, 0.4 A cm^{-2} representing low current density and 1 A cm^{-2} nominal operating current density is presented in Figure 15, taken from polarisation curves measured immediately after every 100 h of FC-DLC and following the 10 h shutdown to quantify cell recovery. Reference cell voltages were measured with pure hydrogen for comparison. A staggered decay is noted, as performance improved slightly after cell shutdown. Cell voltage recovery at 1 A cm^{-2} following the shutdown was generally better in the poisoned cell as compared to the reference cell, with cell voltages recovering by 32.7 mV, 58.5 mV and 91.9 mV after 100 h, 200 h and 300 h respectively (about double of that seen for the reference cell). It should be noted that the shutdown duration after 300 h was extended to about 18 h due to facility complications.

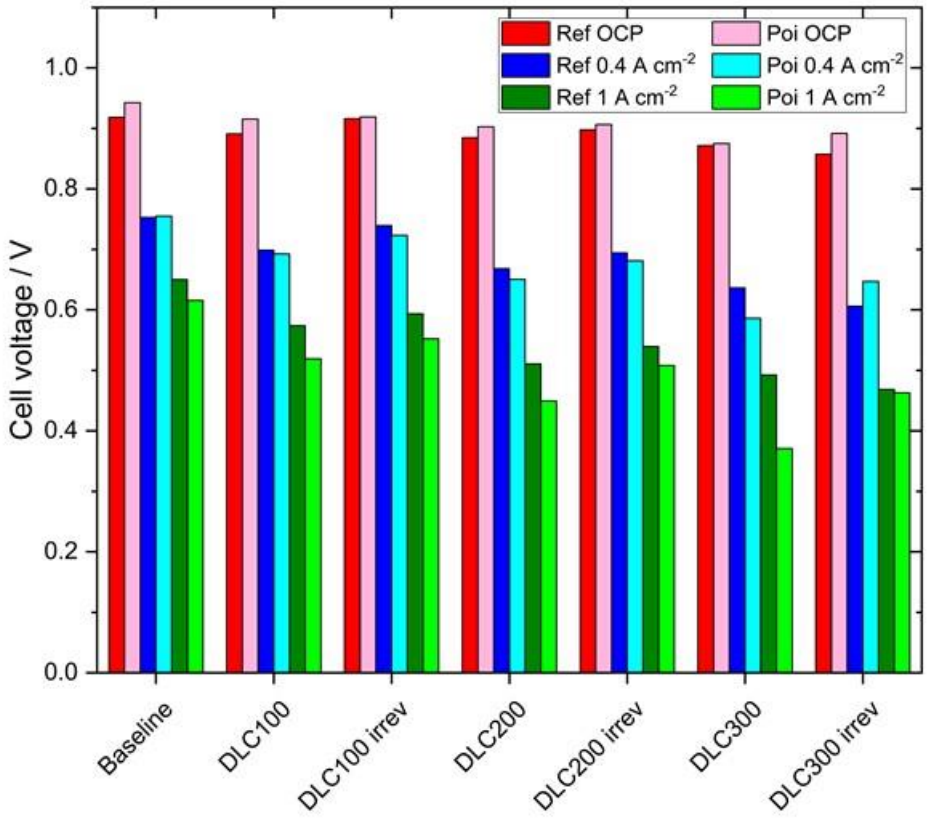

Figure 15 - Cell voltages at open circuit, 0.4 A cm^{-2}, and 1 A cm^{-2} at various phases of testing

Cell voltage decay at 0.4 A cm^{-2} showed the same staggered profile but was more gradual than observed for 1 A cm^{-2}. Open circuit potentials were slightly higher for the poisoned cell compared to the reference but since this was observed during the baseline measurement (before poisoning), it can be attributed to intrinsic cell behaviour rather than the impact of the contaminant mixture on the cell at open circuit.

From Figure 16, it is noted that the recovery (shutdown) period improves cell performance proportionally to the current density applied. Cell performance after recovery almost matches the performance measured 100 h earlier.

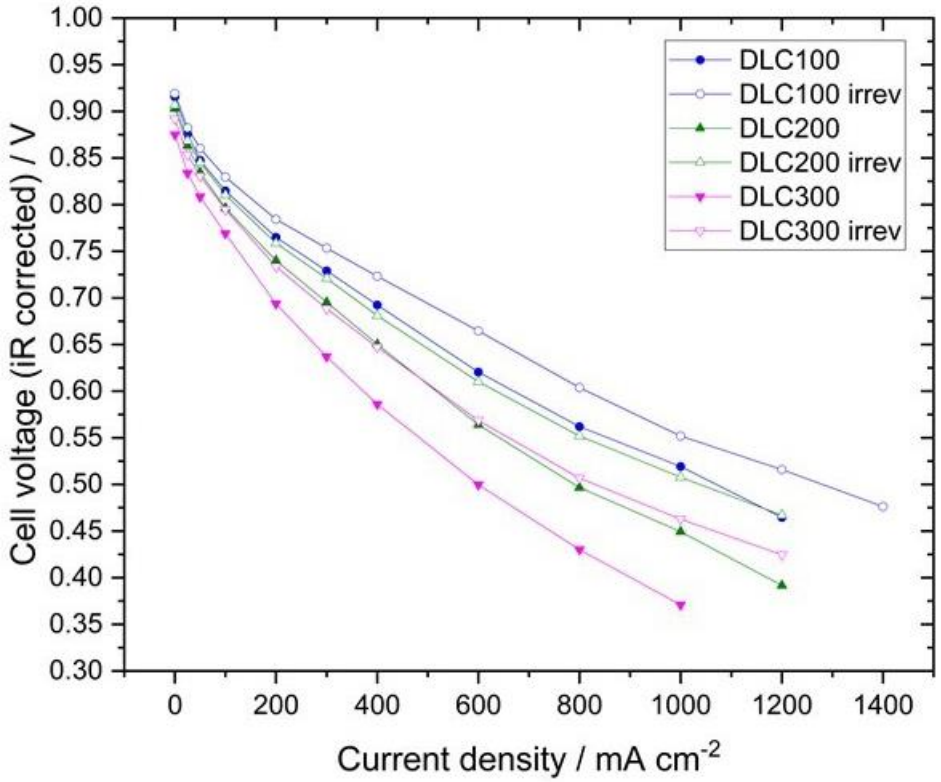

Figure 16 - Polarisation curves measured immediately after FC-DLC and following 10 h shutdown

The electrochemically active surface area (ECSA) of the cathode and anode catalyst was also measured after every 100 h of FC-DLC, following the 10 h recovery shutdown period. From Figure 17, it is clearly noted that the hydrogen contaminant mixture exacerbates the loss in ECSA when running FC-DLC, when compared to the reference values obtained using pure hydrogen.
With pure hydrogen, active surface area on the catalyst appears to decline linearly over 300 h, even showing an improvement in the case of the anode after 200 h. However, with the contaminant mixture the ECSA suffers the biggest decline over the first 100 h, behaviour similar to that observed on the polarisation curves (Figure 14). Beyond the first 100 h, ECSA loss in the cathode seems similar to the cell running on pure hydrogen, while some gain in ECSA was even observed on the anode. The improvement may be due to the extended shutdown and recovery period after 300 h that was mentioned previously, but this remains unknown.

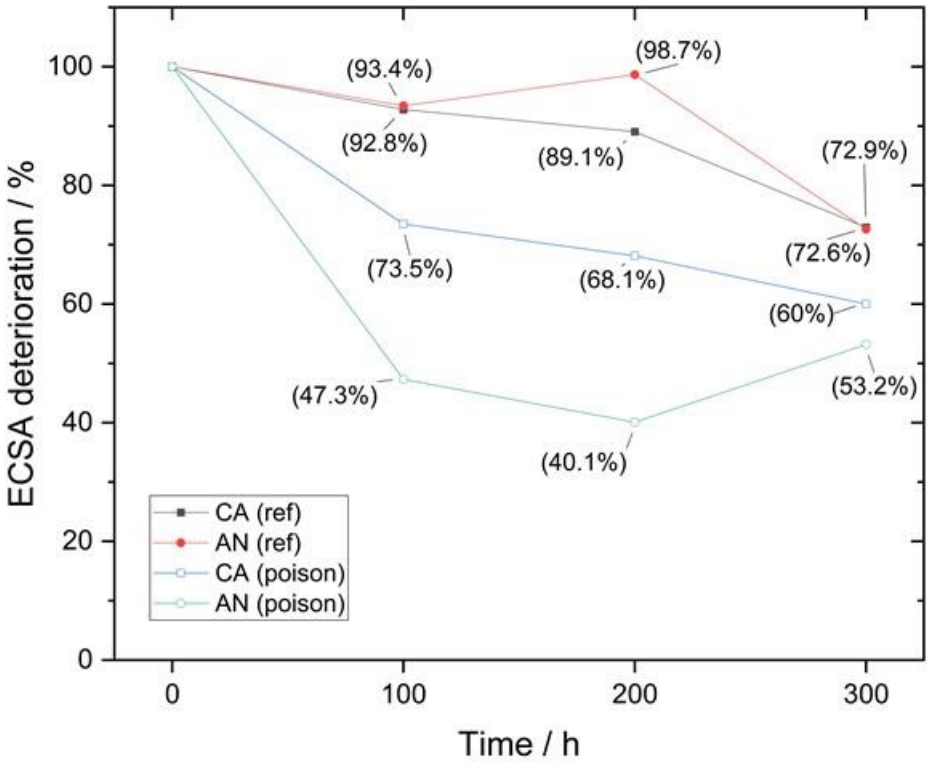

Figure 17 - ECSA deterioration measured every 100 h, from cyclic voltammograms with 50 mV s^{-1} scan rate

4.3 Measurements on Short-Stacks (A3.2.3)

4.3.1 Tests carried out at NPL

NPL and CEA used the same stack, consisting of 8 cells with 220 cm^2 active area MEAs from HyPlat to check the reproducibility of polarization curves obtained at the two institutes. Polarisation curves were measured (Figure 18) following a break in period where the stack was held galvanostatically at 0.5 A cm^{-2}, and a close consensus was noted between the measurements made in NPL and CEA. Cell voltages appear to diverge starting from 1 A cm^{-2} and this is possibly caused by the difference in the humidification methods used. Nonetheless, the short-stack was later operated at 0.7 A cm^{-2} during poisoning for a starting voltage of 0.65 – 0.7 V.

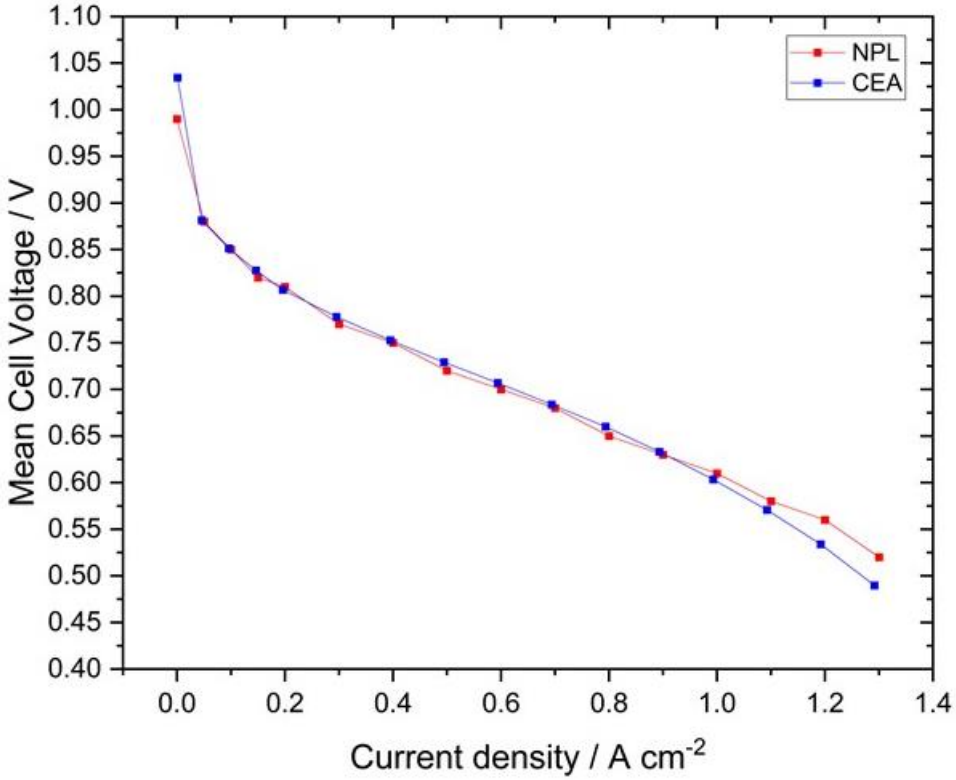

Figure 18 - Polarisation curves measured at BoL at NPL and CEA on the same stack

To establish a reference for poisoning response, the fuel cell stack was first poisoned with CO at 0.2 µmol mol^{-1} (ISO threshold) and 0.8 µmol mol^{-1} concentrations. This step enabled better understanding of the stack tolerance to hydrogen contaminants and provided a good reference measurement for comparison. Following this, the fuel cell was then poisoned with the hydrogen contaminant mixture at concentrations equivalent to 0.2 µmol mol^{-1} and 0.8 µmol mol^{-1} CO.

The evolution of cell voltage during poisoning with CO (reference) and the hydrogen contaminant mixture is presented in Figure 19. In both tests with 0.2 µmol mol^{-1} CO and 0.2 µmol mol^{-1} CO equivalent in the contaminant mixture, cell voltage remained steady with less than 1 mV of decay noted over the 4 h test period. Likewise for the 0.8 µmol mol^{-1} CO and 0.8 µmol mol^{-1} CO equivalent contaminant mixture, cell voltage deterioration began quickly and was continuous throughout the same duration; cell voltage decay appeared to be slower for the first 2 h before deteriorating more rapidly, resulting in a total loss of approximately 14 mV in 4 h.

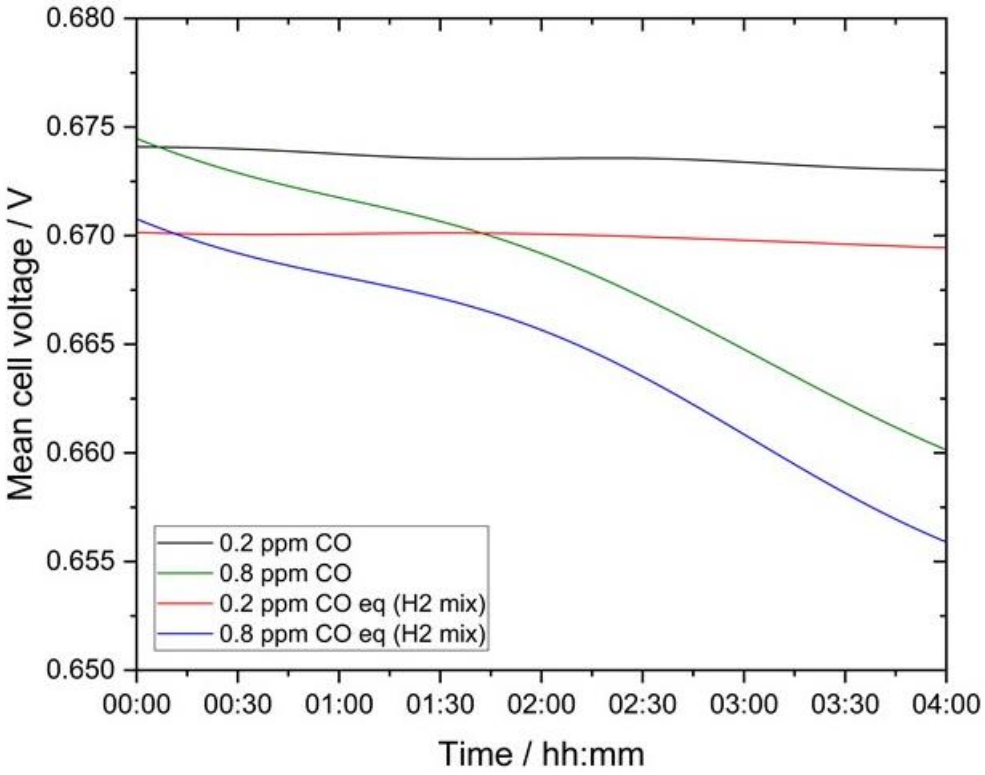

Figure 19 - Cell voltage decay on the short-stack during 4 h poisoning with the hydrogen contaminant mixtures and CO reference mixtures

4.3.2 Tests carried out at CEA

The first test on the short-stack at CEA was done after conditioning with a polarisation curve in the nominal conditions. This test allowed to check both performance expected regarding the selected technology and to check correct stability of applied operating conditions on the test bench (temperatures, pressures and stoichiometry for both Hydrogen and Air shown on Figure 20 - Polarisation curve in nominal conditions at BoT. Average voltage, operating conditions and individual cells voltage.) in the through flow mode with stoichiometric control. Stoichiometry data are confirming 0.2 A/cm² as the minimum current density below which flow rates are kept constant, as needed to properly operate and control the pressures. Small variations observed on the controlled conditions of flow rates, temperatures or pressures are indeed far below values affecting the performance.

The individual cells present similar voltages with a maximum gap lower than 25 mV at the maximum current density tested (here 1.4 A/cm²) for the 7 cells not including the additional resistance of the segmented cell plate. The cell #5, hence the cell voltage U5 is lower consistently with the ohmic drop caused by the segmented cell plate on the measured voltage. These data present good enough homogeneity among cells in the nominal conditions confirming valid and state of the art performance of the tested stack for this technology.

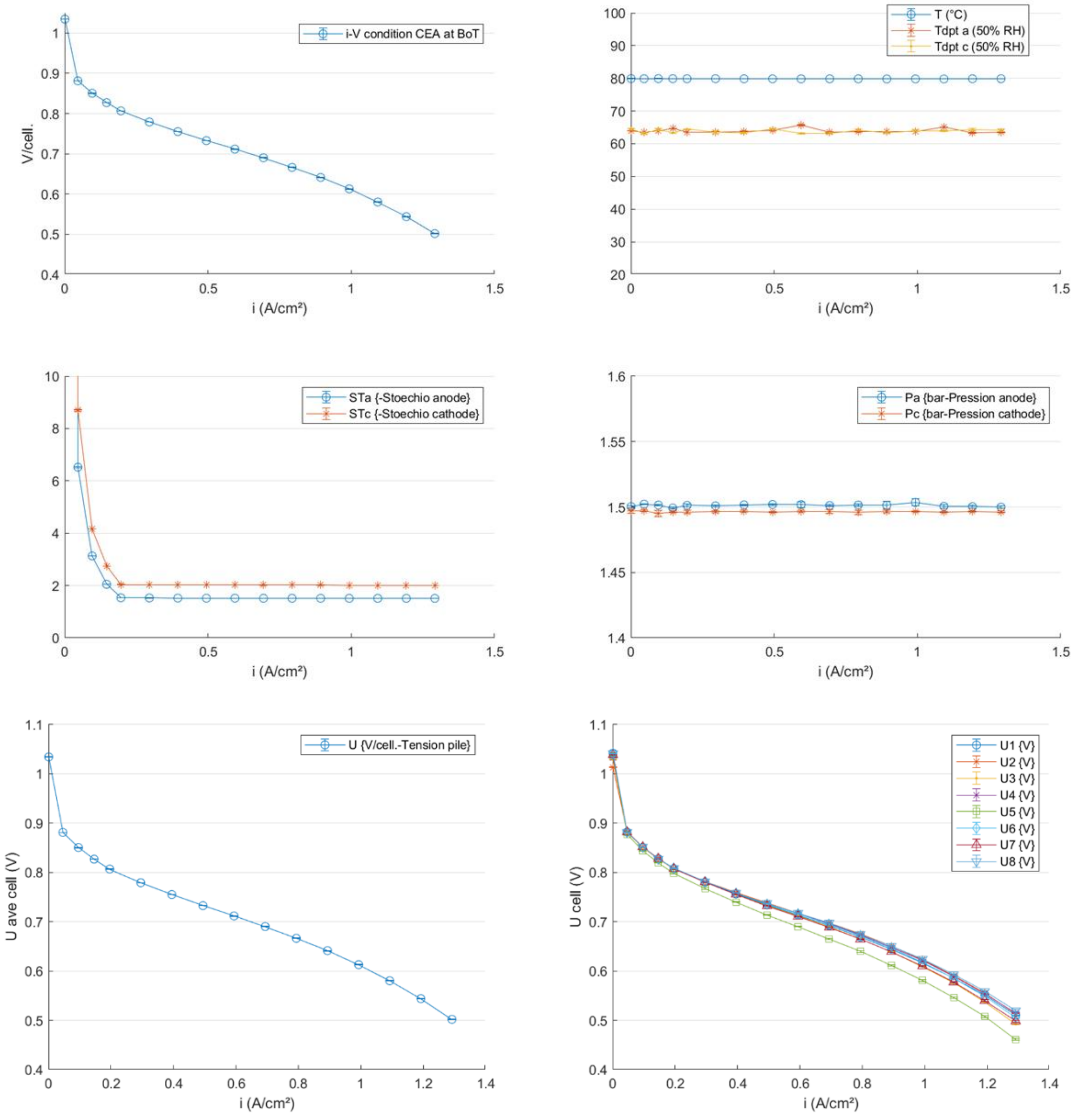

Figure 20 - Polarisation curve in nominal conditions at BoT. Average voltage, operating conditions and individual cells voltage.

Additional electrochemical characterization were performed in order to measure anode and cathode electroactive surface areas. Cyclic voltamograms in Figure 21 were recorded at beginning of test showed similar behaviour for all cells, with higher active surface area cathode side, consistent with the catalyst layers loadings of 0.1 mg_{Pt} cm^{-2} (anode) and 0.4 mg_{Pt} cm^{-2} (cathode). These data confirm that MEA in cell#5 presents same properties as the others.

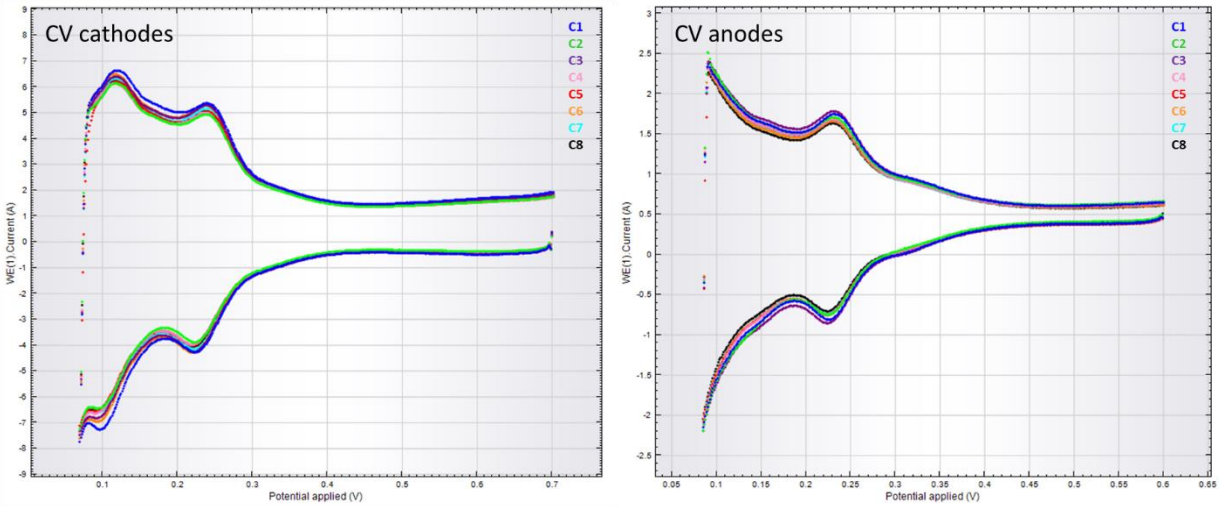

Figure 21 - Cyclic voltammograms recorded at 0.1 V/s at BoT on all cathodes (left side) and all anodes (right side) of the 8-cell stack tested at CEA at the beginning of life.

4.3.2.1 Beginning of test performance of the short-stack measured in recirculation mode

Next results presented are part of the reference test conducted before impurity testing.

Two polarisation curves have been performed in, and after stabilisation in, operating conditions selected for the assessment of tolerance to an impurity, namely: recirculation mode anode side with regular purges as described in the experimental section. Same information are given in the Figure 22 for two repeated experiments (7 h and 12 h of operational time after start-up): the average voltage (top left), the stack temperature and two gases dew points at stack inlets (top right), stoichiometric ratios (bottom left) and pressures (bottom right) for anode and cathode sides.

Results showed good repeatability. For similar operating temperature, stoichiometric ratios and pressures, recirculation mode, which leads here particularly to lower humidification on the anode side (dew point only slightly higher than 20 °C at anode inlet without direct humidification of the Hydrogen), causes slightly lower performance compared to nominal flow through mode. The difference in performance is however mostly noted at the higher current density, with average voltage at 1.2 A/cm² similar to voltage measured at 1.25 A/cm² in nominal conditions.

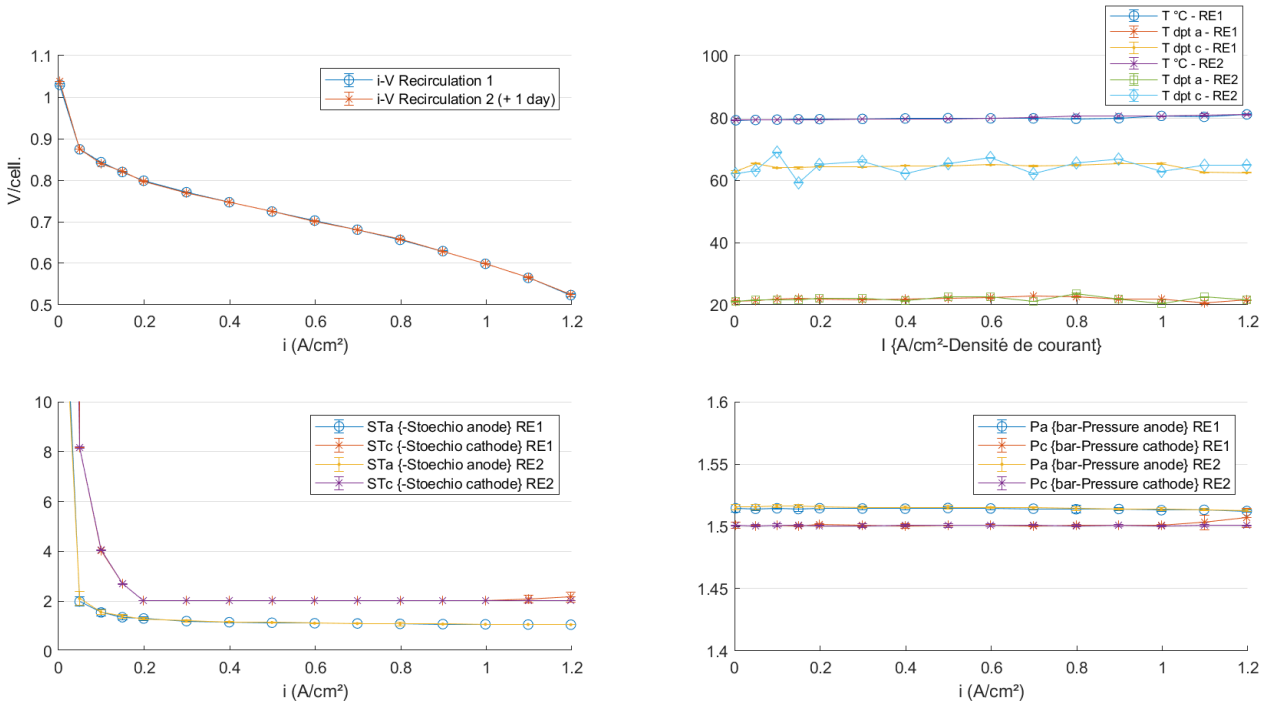

Figure 22 – Initial polarisation curves in recirculation + purges mode at BoT. Average voltage and operating conditions.

4.3.2.2 Impact of CO impurity during daily poisoning tests (mixtures 0.8 ppm CO + Hydrogen)

The aim of this test was to check the tolerance to low content of CO during a daily experiment including always same start-up procedure and stabilization under pure Hydrogen of more than one hour before shifting to mixture. The stack was poisoned using directly mixtures prepared with 0.8 ppm CO in Hydrogen. 0.8 ppm was selected to get significant impact during the duration of 90 minutes poisoning.

During the test, CO content was measured in the recirculation loop by an analyser based on IR (PROCEAS type): these measurements showed that much less than 0.8 ppm CO is present in the recirculation loop confirming adsorption of some CO within the stack. Only about 0.12 to 0.23 ppm are measured during 90 min of poisoning. Hydrogen flow rate, proportional to the current in the stoichiometric mode, has a major influence on the CO fed into the stack and adsorbed. As a result, CO content in the flow was mostly imposed by the current with about a ratio of 1.5 - 1.6 between CO measured in the loop for 220 A vs. 132 A. One case allowed to show what happens when adsorption of CO reaches a coverage threshold: the content increases, here up to 0.4 ppm, meanwhile average voltage drop is accelerated.

Voltage loss was assessed and compared after same duration of 90 min after switching from pure Hydrogen to mixture with CO (Figure 23). The voltage drop is higher when operating the stack at higher current of 1 A/cm² vs. 0.6 A/cm² (about 100 mV difference in corresponding voltages) and at lower temperature.

At lower current tested of 0.6 A/cm², voltage loss of few mV is slightly higher compared to NPL data (obtained at 0.7 A/cm²) but still results are consistent and in the same range.

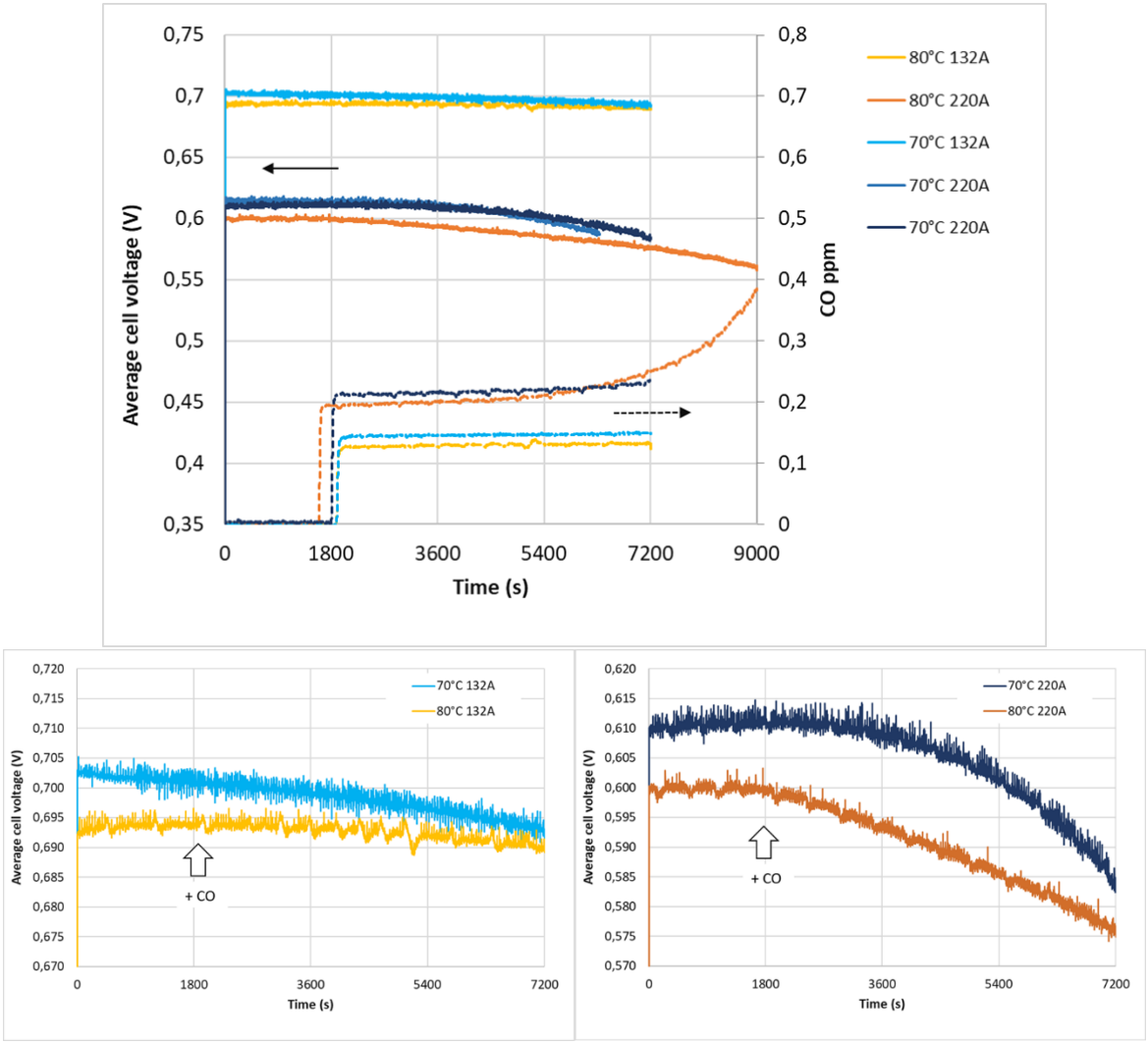

Fixed conditions	Test #1	Test #2	Test #3	*Test #4*	Test #5
H2 Recirculation 10Nl/min Purges 0,5s each 60s P H_2/air =1.5/1.5 bara St Air = 2 RH = - / 50%	T=80°C 132A	T=80°C 220A	T=70°C 132A	*T=70°C* *220A*	T=70°C 220A
Voltage loss in 90 minutes	4 mV	24 mV	8 mV	*NA*	28 mV
CO measurements	Yes	Yes	Yes	*No*	Yes

Figure 23 - Voltage decrease and CO measured online by sampling from the recirculation loop during poisoning tests with 0.8 ppm CO in Hydrogen – Impact of temperature at two current levels corresponding to 0.6 and 1.0 A/cm².

These results confirmed, as mentioned in the methods section, that the selection of current and operating conditions has a significant influence on the assessment of impurities' impact.

4.3.2.3 Impact of shut-down procedure on CO tolerance (5 ppm CO)

As described in the methods section, several tolerance tests were performed following a pre-established reference procedure, including start-up, operation under a recirculation mode, stabilization under pure Hydrogen, and switching to mixture of Hydrogen with 5 ppm CO. 5 ppm CO was selected to get significant and rapid information, allowing to repeat the poisoning twice, while including a shut-down and restart procedure, in one single-day experiment.

These tests aimed at checking the role of air cleaning during shut-down procedure after a first poisoning by CO, in order to confirm the importance of controlling this step for measurements targeting impurities' impact assessment.
Experiments presented in Figure 24 allowed to check the effect of a specific shut-down procedure defined in the projects Hydraite and MetroHyve2. The procedure includes a period with some air feeding into the anode side, in order to actually remove the traces of CO adsorbed on the catalyst, after the decrease of current and stop of hydrogen flow. The effect of long stop (off periods namely corresponding here to nights or week-ends) could also be checked: it appeared that this type of stop could probably also allow some air into the stack including the anode side, hence also leading to a anode catalyst surface cleaning. However systematically applying a shut-down with air cleaning is recommended as it is controlled and allows reliable assessment of impurities' impact afterwards.

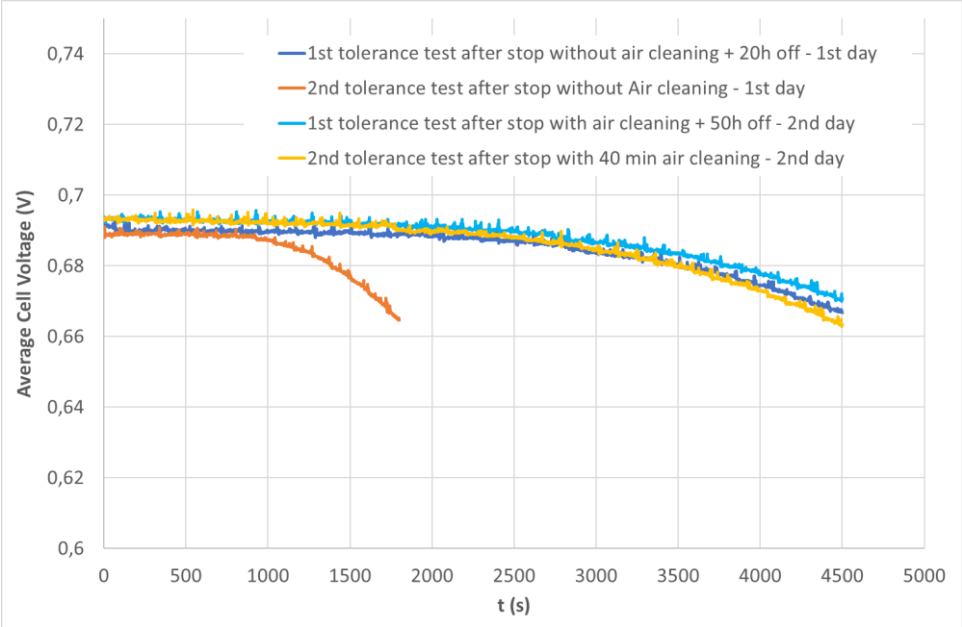

Figure 24 - Voltage decrease during CO tolerance tests – Impact of shut-down procedure with or without air.

Results presented in Figure 25 correspond to daily experiments with again 2 successive tolerance tests, showing different poisoning impact of the 1st one, and performed after shut-down with air cleaning for the 2nd one. The data are confirming the actual effect of air cleaning during shut-down procedure for different cases of pre-poisoning.

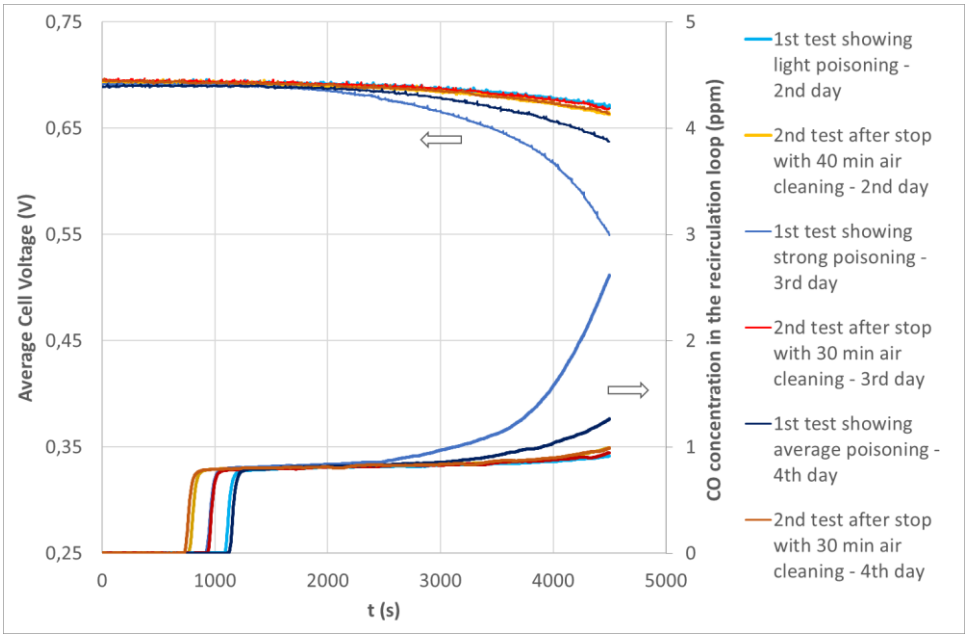

Figure 25 - Voltage decrease and CO measured online by sampling from the recirculation loop during CO tolerance tests.

These results with two successive tolerance tests are confirming the importance of controlling the status within the stack regarding particularly the previous poisoning of the catalyst surface. Here it is shown that at least applying a clearly defined cleaning procedure allows to get reliable result regarding the impact of impurities.

4.3.2.4 Impact of FC-DLC on CO tolerance

Experiments reported below (load cycles and tolerance to poisoning by 5 ppm CO) are conducted in nominal conditions (80 °C, 1.5 bars, 50 %RH and st 2 for the air side; always recirculation mode for Hydrogen side).

Note: data of cell #5 are affected by the resistance of the segmented plate.

Results below showed that voltage losses are caused by 100 h of dynamic load cycles. Non-reversible voltage losses of about 20 mV at operating point of 0.6 A/cm² were similar for the operation under pure Hydrogen and during poisoning with 5 ppm CO. The tolerance during the 2nd poisoning test was identical before and after the ageing. Performance losses are thus related to the overall operation and possible degradation of the stack and MEAs with no specific effect on the tolerance to impurity on the considered short time frame.

When considering the 1st poisoning test just after the load cycles, the voltage decrease is almost similar to the previous experiment conducted the day before starting the cycles, even if the initial voltage (before adding CO) is 30 mV lower.

The conclusion is that 100 h of load cycles initially caused about 30 mV performance loss, kept identical when adding CO. Stop after 1st CO poisoning allowed to recover part of the losses. The sensitivity to impurities was not affected on the global voltage, nor on the individual cells voltage.

Analyses of local data could help to check if this short-term ageing had an effect on the poisoning along the surface of the MEAs.

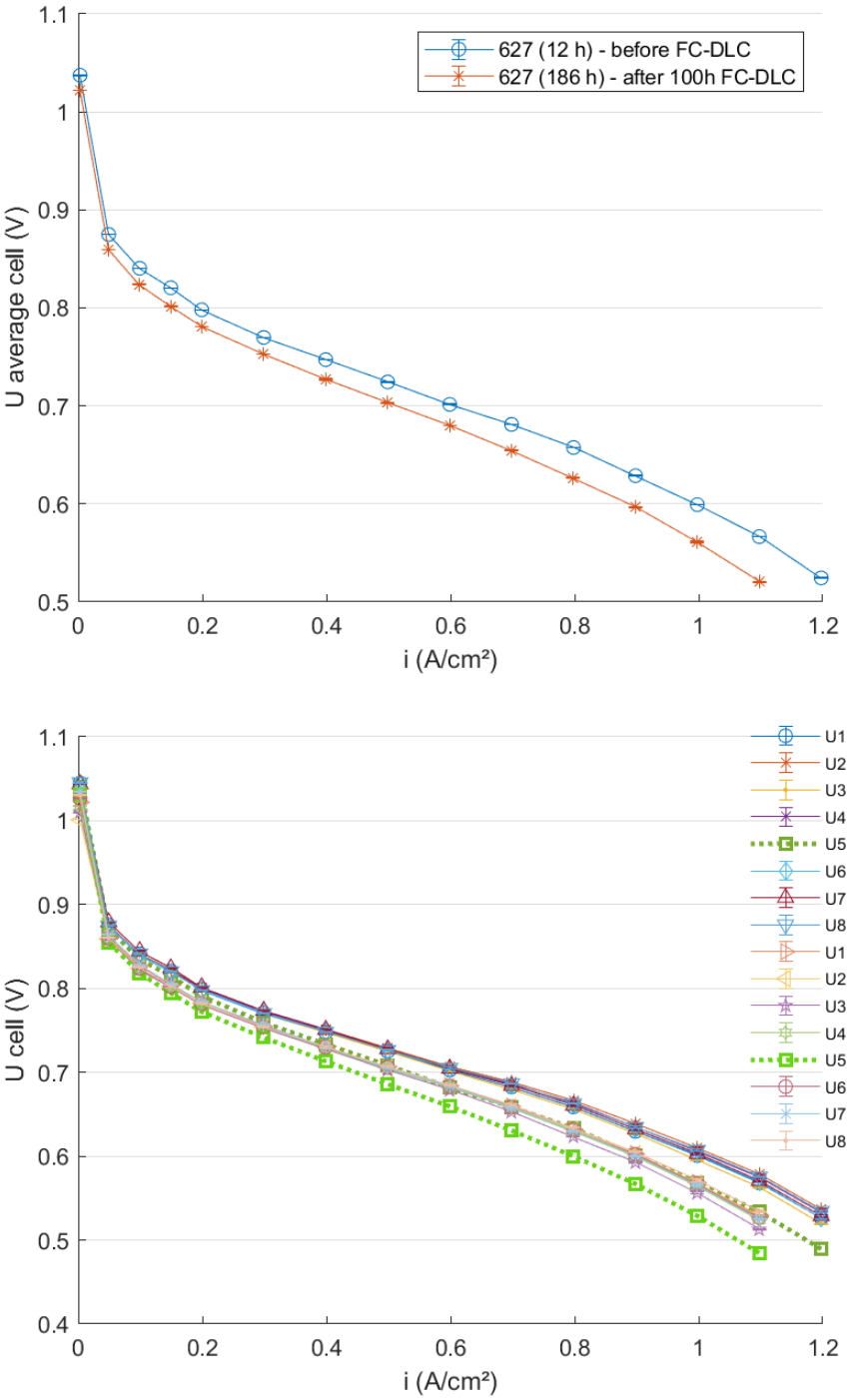

Figure 26 : Polarisation curves (stack average voltage and all cells voltage) before and after a period of 100h operation in FC-DLC mode.

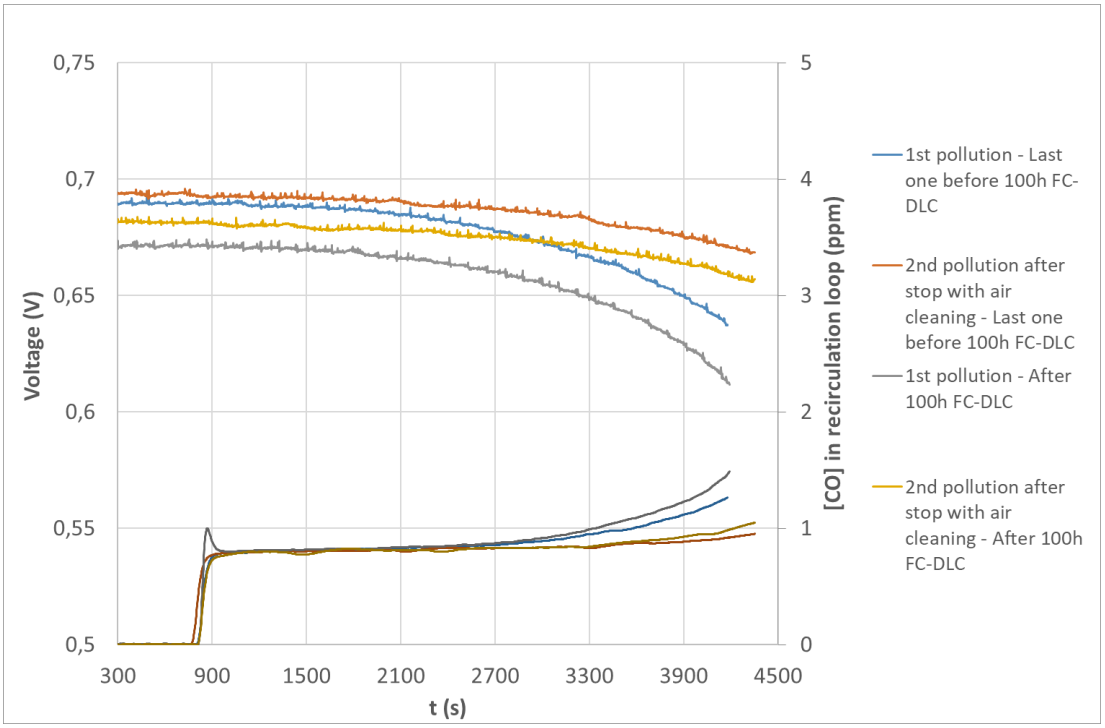

Figure 27 - Voltage decrease and CO measured online by sampling from the recirculation loop during CO tolerance tests with 5 ppm CO at fixed current density of 0.6 A/cm², before and after a period of 100h operation in FC-DLC mode.

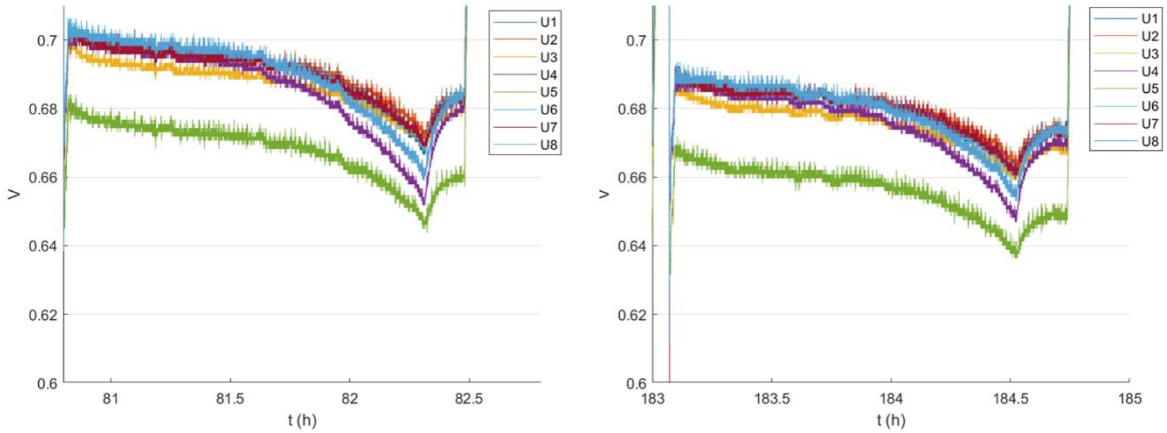

Figure 28 - Cell voltage decrease during 2nd CO tolerance tests with 5 ppm CO at fixed current density of 0.6 A/cm², before (left) and after (right) a period of 100h operation in FC-DLC mode.

4.3.2.5 Local current density measurements to analyse the impact of CO poisoning.

Figure 29 is describing the information obtained with the segmented device (S++® card) placed in the middle of the stack between cells 4 and 5, which are current density distribution maps (CDDM). The current density distribution can give information about the heterogeneities along the cells surface with the zones presenting better or lower local performance, and about the modifications of these heterogeneities when operating conditions are varied, including when impurities are added. In the results presented, difference calculated between two CDDM is often used to enhance the variations between two situations (between two stabilized conditions or before/after an event in same conditions).

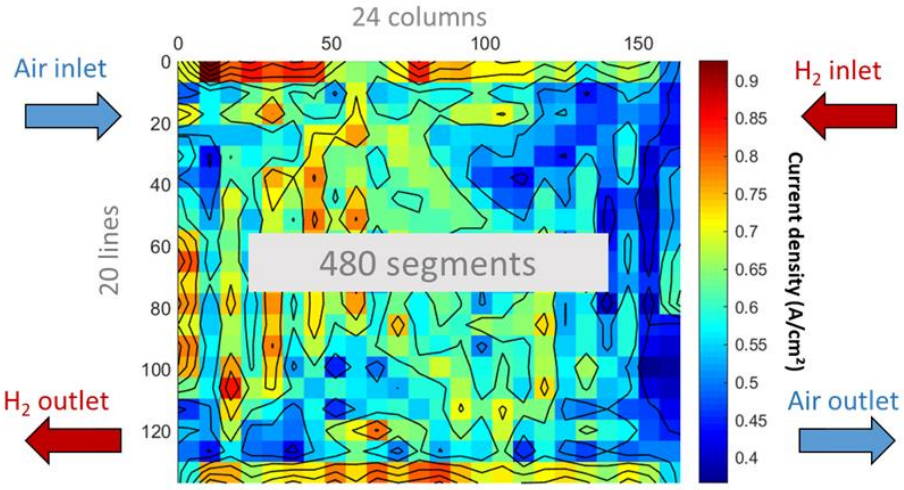

Figure 29 - Scheme of a Current Density Distribution Map (CDDM) obtained with measurements on 480 segments. Are also indicated on this figure the zones corresponding to Air and Hydrogen inlets/outlets, the coloured range of current density values.

The local impact of poisoning the hydrogen with 5 ppm CO is illustrated in Figure 30 with the evolution of the CDDM during the tolerance test. On the original CDDM, it appears that more current density is always produced in the half zone near the air inlet, showing major impact of oxygen concentration on the distribution of current.

When CO is added, the CDDM is not immediately modified, but after some time, the concentration of higher current densities is even more shifted towards air inlet part of the cell, meanwhile, the part of the cell with lower current densities is extended from the Hydrogen inlet zone towards the middle. It is particularly interesting to note that if the impact of poisoning on the CDDM starts with a significant delay after adding CO, it is maintained after stopping the poisoning, by switching from the mixture to pure Hydrogen again (indicated as “Stop CO” on the figures).

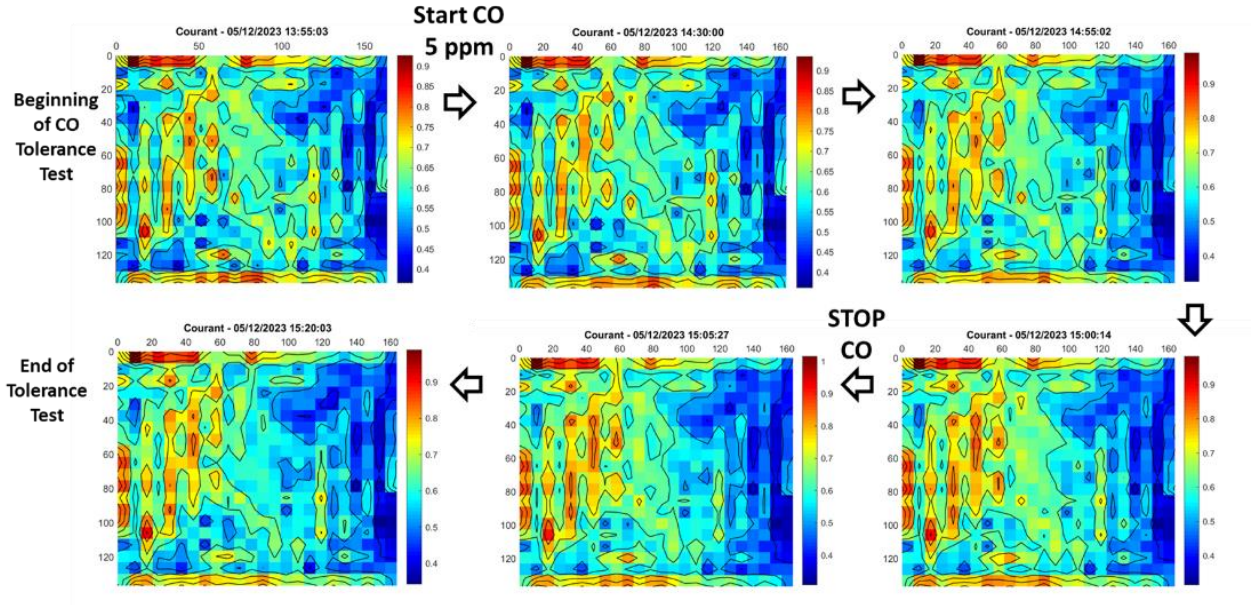

Figure 30 - Current density distribution maps measured using a segmented plate (S++®) placed in the middle of the stack. CDDM reported at different times during a CO tolerance test from BoT until the EoT, indicating the moments when the shift is performed between pure Hydrogen to mixture with 5 ppm CO (= START CO) and the reverse (= STOP CO).

All the phenomena described during the poisoning process along the cell surface are strongly exacerbated and more visible on Figure 31 with the difference between CDDM at a moment and the last CDDM before adding CO. After a duration corresponding to a threshold in the coverage process of the anode catalyst by CO, two distinct zones appear clearly with current densities becoming much lower versus initial distribution (where the difference is positive (red) meaning that initial currents were higher). This occurs on the Hydrogen inlet side, where the CO is more likely able to primarily accumulate, particularly with the recirculation mode applied during these poisoning experiments.
The CDDM evolution in Figure 32 presented in conjunction with the average voltage during the poisoning test shows how the performance is actually more strongly affected with an acceleration in the voltage decrease when the threshold of adsorption is approached (2 clear zones blue / red on the CDDM differences). This moment also consistently corresponds to the increase in CO content detected on the samples from the recirculation loop.

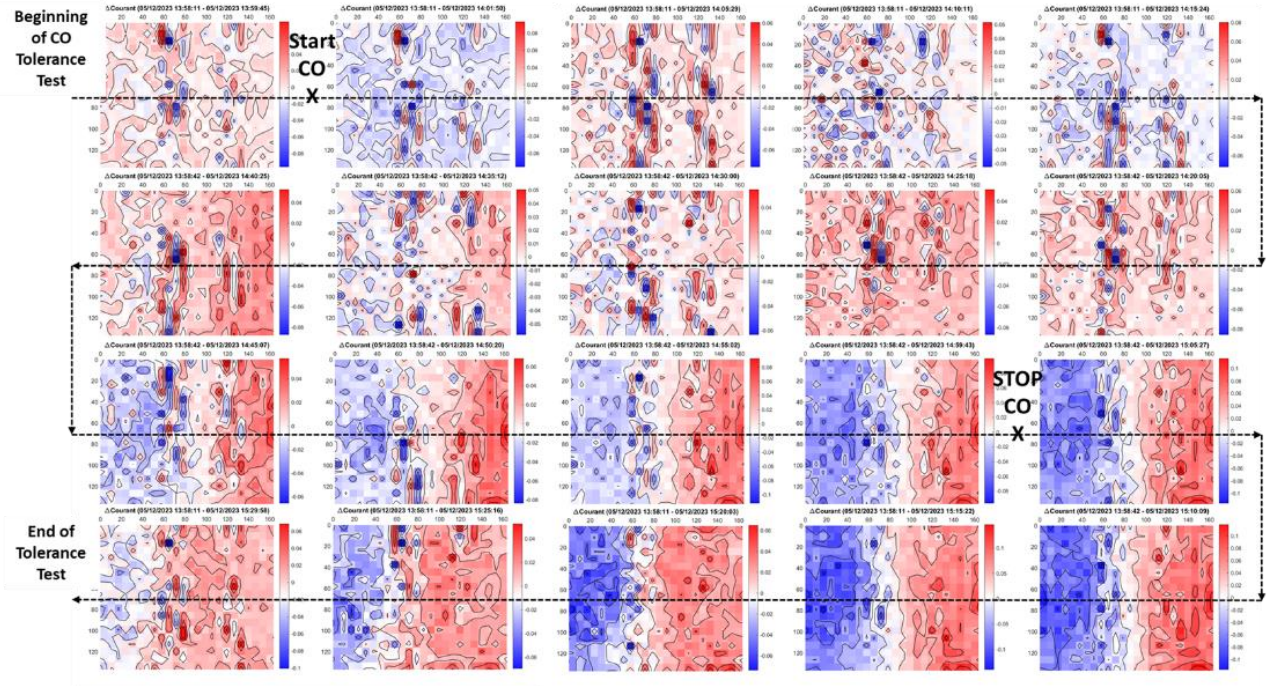

Figure 31 - Relative CCDM vs. CDDM at BoT. Difference reported at selected times during a 5 ppm CO tolerance test from BoT until the EoT, indicating the moments when the shift is performed between pure Hydrogen to mixture with 5 ppm CO (= START CO) and the reverse (= STOP CO).

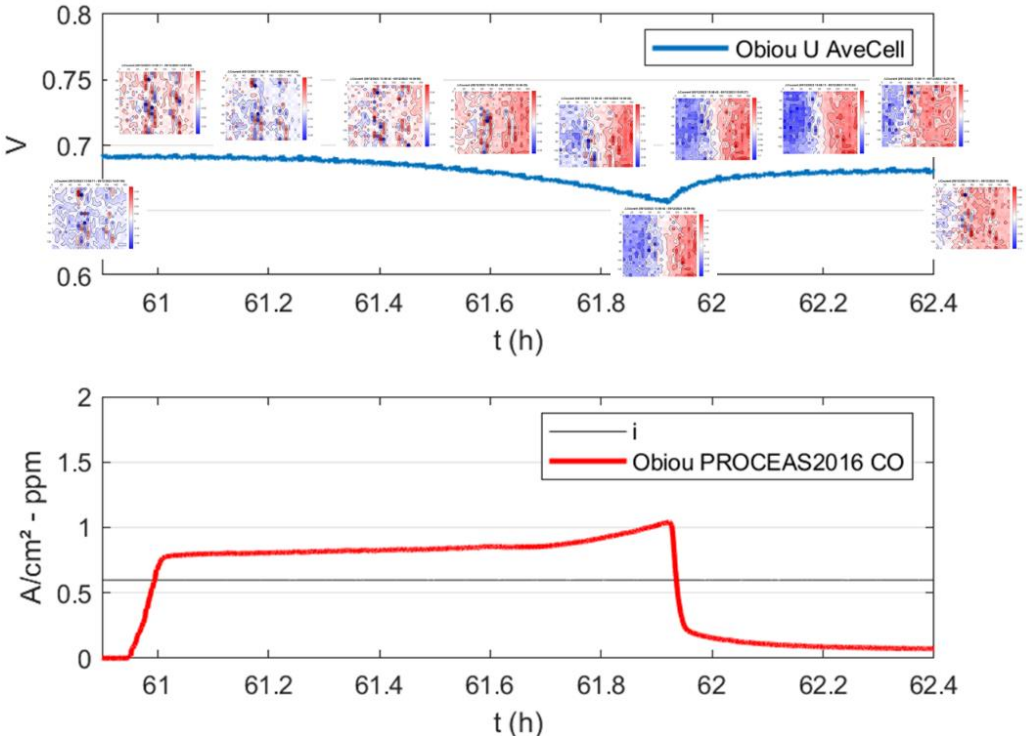

Figure 32 – Evolution of average cell voltage with relative CDDM images during reference poisoning tests (top graph). Current density (grey line) and CO content measured in the recirculation loop during H_2 + 5 ppm supply (bottom graph).

4.3.2.6 Local current density measurements to compare the impact of CO poisoning before and after load cycles.

The experiments and data treatment presented above have been repeated before and after the 100 hours period of dynamic load cycles. When considering the evolution of CDDMs during the second tolerance test in both cases, with the voltage and the CO contents, information look globally similar before and after load cycles (see Figure 33).

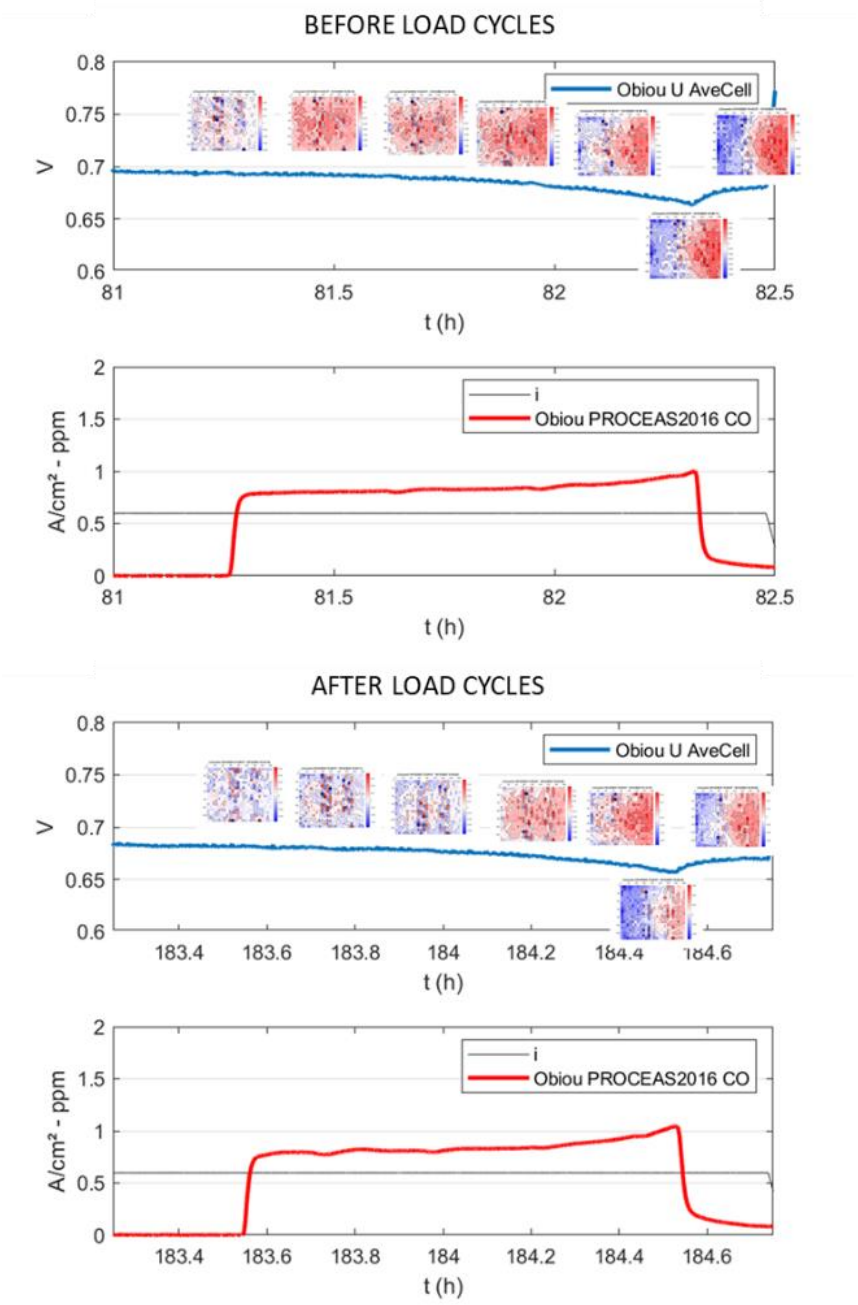

Figure 33 – Average cell voltage with images during time of the differences between CCDM at a time and the CDDM at BoT (top graph). Current density with CO content (bottom graph). Data during the second tolerance tests the day before cycles and the day after cycles.

Full experiments are described with additional information in Figure 34 to show the two successive tolerance tests (poisoning by 5 ppm CO) applied the day before and the day after the load cycles. As already commented on the performance data, the 1st tolerance test was in both cases more aggressive.

When considering the current density distribution, it appears that the contrast between the two zones is slightly higher before / after the first tolerance test, while the low tolerance zone (red part) is slightly extended before / after the 2nd tolerance test.

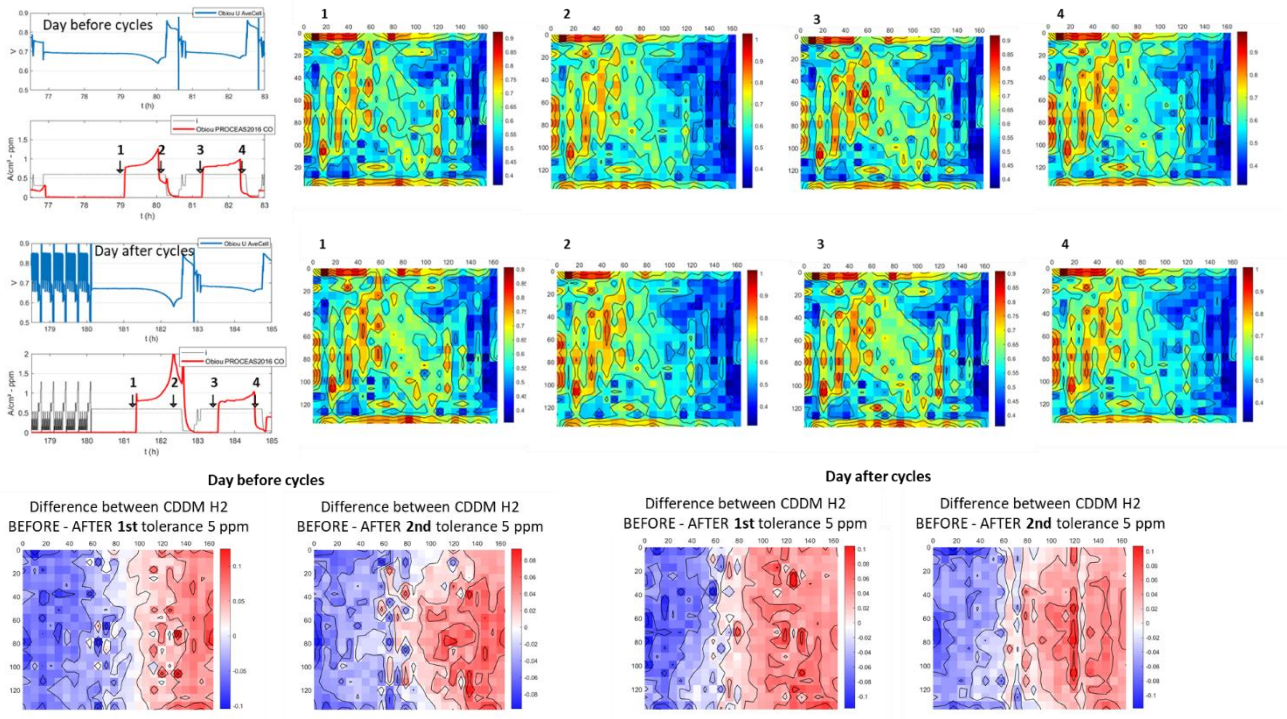

Figure 34 - Average cell voltage, current density with CO content during experiments the day before cycles and the day after cycles. CDDM images and differences between CCDM before / after CO tolerance tests for the different cases.

In Figure 35, local performance before poisoning are slightly better on most zones before the load cycles (Bb – Ba >0), while just after poisoning they slightly lower on most zones before load cycles (Ab – Aa <0). Locally the tolerance to CO could have been slightly improved. However the differences before and after the 100 h load cycles are not so significant (in the range of +/- 0.03).

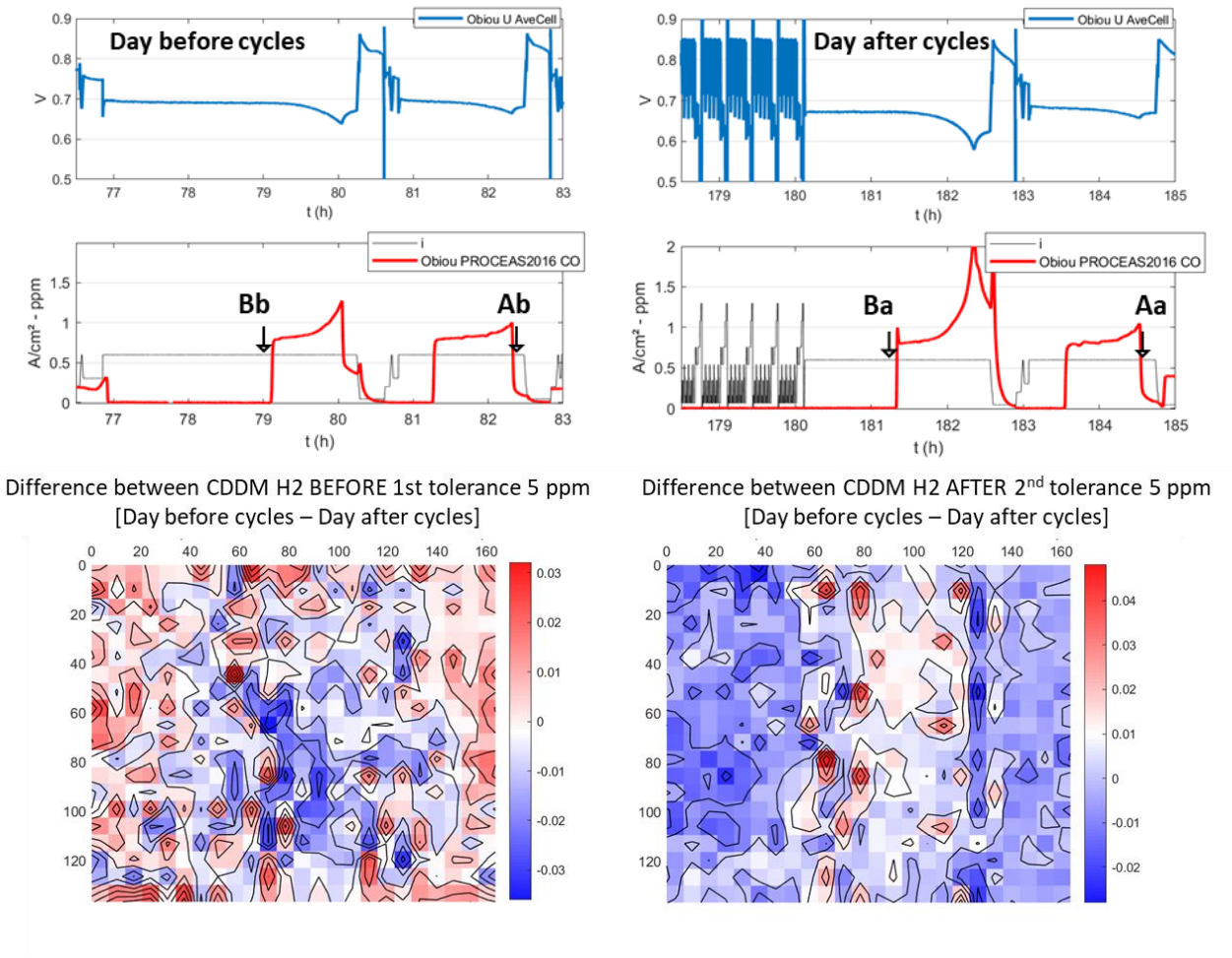

Figure 35 - Average cell voltage, current density with CO content during experiments the day before cycles and the day after cycles (top). Differences between CCDM day before / day after cycles at two moments: before 1st tolerance test and after 2nd tolerance test.

4.3.2.7 Electrochemical characterization by cyclic voltammetry at EoT

Cyclic voltammograms recorded at end of test were compared to beginning of test in Figure 36. Cathode data showed a decrease in active surface area consistent with the performance losses observed on the polarisation curves or at fixed current density without or with CO added in the Hydrogen. Anode side, the cyclic voltammograms seem more modified but there is mainly a translation with an overall baseline current higher at beginning of test, that might be due to some residual hydrogen within the cells during the measurements. Other features of the anode CV seem indicating a modification of the catalyst structure more than a stronger loss of active surface area compared to the cathode side. More electrochemical or microstructure analyses along with more information on the catalyst would be requested to go further in the interpretation.

These data confirm that MEAs were affected by the performance, tolerance and load cycle tests conducted even if total operational time was only about 200 hours.

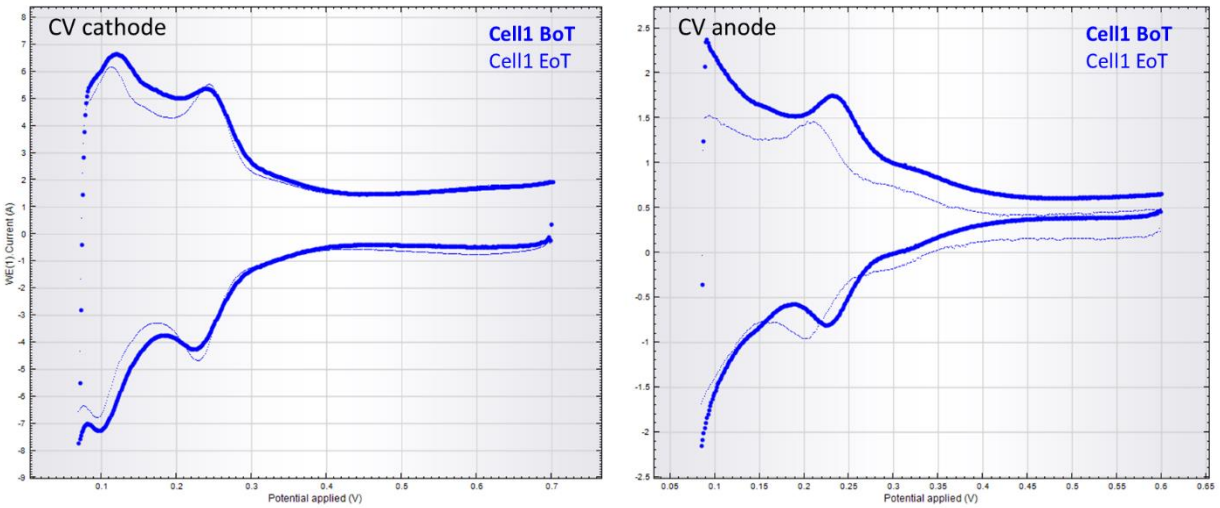

Figure 36 – Cyclic voltammograms recorded at 0.1 V/s compared at BoT and EoT on cell#1 cathode (left side) and anode (right side) of the stack tested at CEA.

5 Results on Air Contaminants (A3.3)

5.1 Single Cell Tests at NPL

When exposed to the air contaminant mixture at 2 % concentration to fulfil the low range test specification on Table 4, the cell voltage immediately decreased continuously, corresponding to a voltage decay rate of approximately 102 mV h^{-1}. The rate of voltage decay began to plateau in the next 1.5 h (~68 mV h^{-1}) before the test was stopped as cell voltage approached the operating safety limits. Figure 37shows the repeatability of results and the trend mentioned. Unfortunately, due to minimum flowrate limitations on the flow controller used, a lower concentration of the contaminant mixture could not be tested.

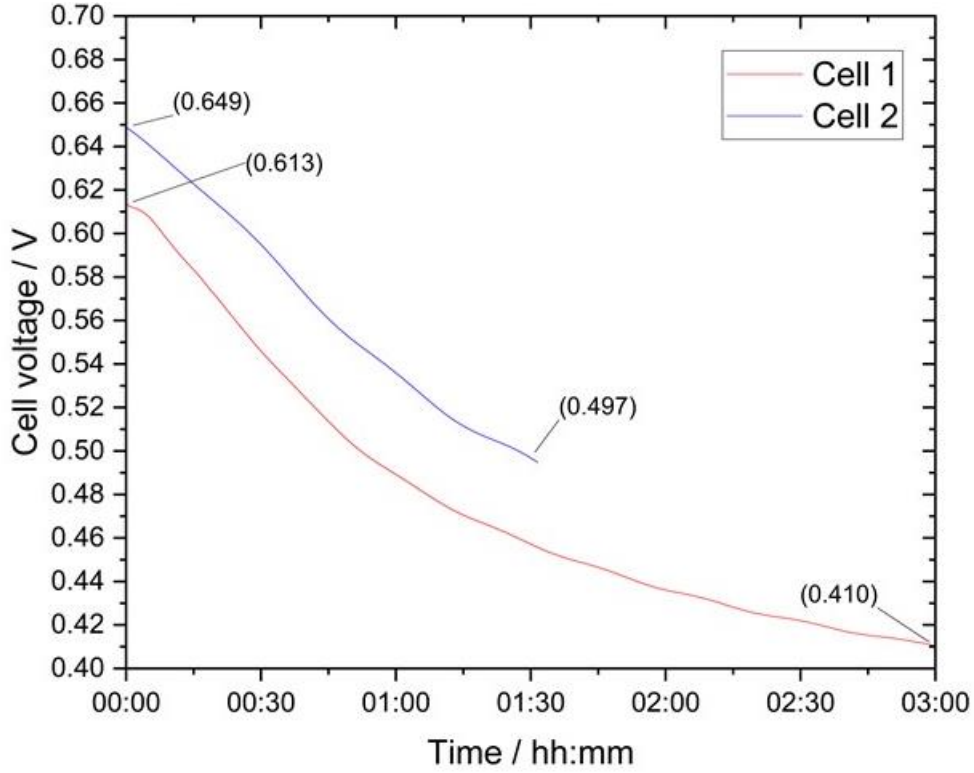

Figure 37 - Single cell PEMFC degradation profile with 2 % air contaminant flow

Previous work by Talke et. al. [2] showed that ammonia at 5 µmol mol^{-1} and NO at 10 µmol mol^{-1} individually caused voltage decay up to 12 mV h^{-1} and 2 mV h^{-1} only when the fuel cell was operated at high current density (1.5 A cm^{-2}). It is likely that the chosen compounds in the mixture were not compatible and had interacted within the cylinder. Considering the extensive voltage decay noted with only 2 % concentration of the air contaminant mixture, no further tests were performed (5 % or FC-DLC) neither at stack level nor with analytical testing (A3.3.1).

5.2 Single Cell Tests at CEA

The performance obtained with the commercial MEA are presented in the 4 different testing conditions proposed in the Table 5 (Break-In, CEA, ASC, EUH). In the aim to study the effects of impurities at very low concentrations, the purity of the gases traditionally available must be verified.
Three different gas purity conditions have been proposed for these reference tests. First, highly pure gases will be tested with hydrogen 6.0 (99.9999%) at the anode and a mixture of nitrogen 6.0 and oxygen 5.8 to create synthetic air. In a second time, the pure hydrogen will be replaced by standard technical H_2 4.5, which is the commonly used purity in fuel cell testing at CEA, while the same synthetic air will be used at the cathode. Lastly, compressed air, made on site at CEA (detailed purity unknown), will replace the synthetic air to obtain reference gas purity conditions.

5.2.1 Polarisation curves under different gas purities

As stated above, three gas configurations have considered here:

- Hydrogen 6.0 / Synthetic Air (N_2 6.0 + O_2 5.8);
- Hydrogen 4.5 / Synthetic Air (N_2 6.0 + O_2 5.8);
- Hydrogen 4.5 / Technical Air (lab gas network used as reference supply).

The different polarisation curves obtained for the three gas configurations under the 4 different conditions are presented respectively on Figure 38 to Figure 41. The current density of both Break-In and CEA conditions is around 25 % lower than the ASC and EUH conditions at 0.5 V. This is mainly due to lower reactant pressures. In the break-In conditions, the cell appears to operate better than in the CEA conditions simply because of the higher relative humidity (80 *vs*. 50 % RH). No real difference in terms of performances can be observed between ASC and EUH conditions.

Regarding the impact of gas purity, it appears that the performances are very similar for the 4 tested conditions over the whole current range. One exception can be though observed under Break-in conditions at high current density (above 1.2 A/cm²) and the performance is not related with the gas purity. This gap in cell performance is likely due to thermal effects. Indeed the single cell hardware is not cooled actively and the regulation of cell temperature can exceed the 80 °C set point with then impact the RH and water management in the cell.
As a conclusion regarding short-term operation, reference gas purity (Hydrogen 4.5 and technical Air) can be used to characterize the performance level in single cell configuration.

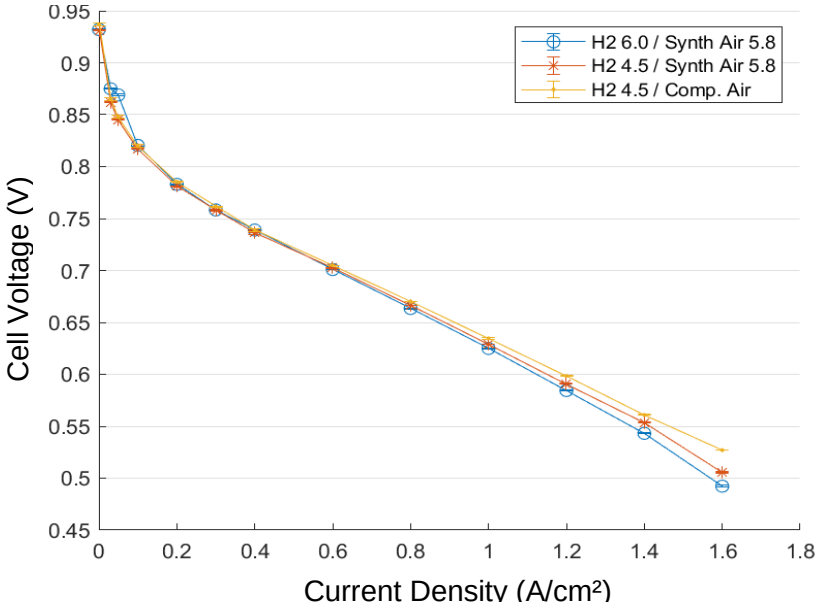

Figure 38 - Polarisation curves at beginning of life for the three gas combinations in Break-in conditions

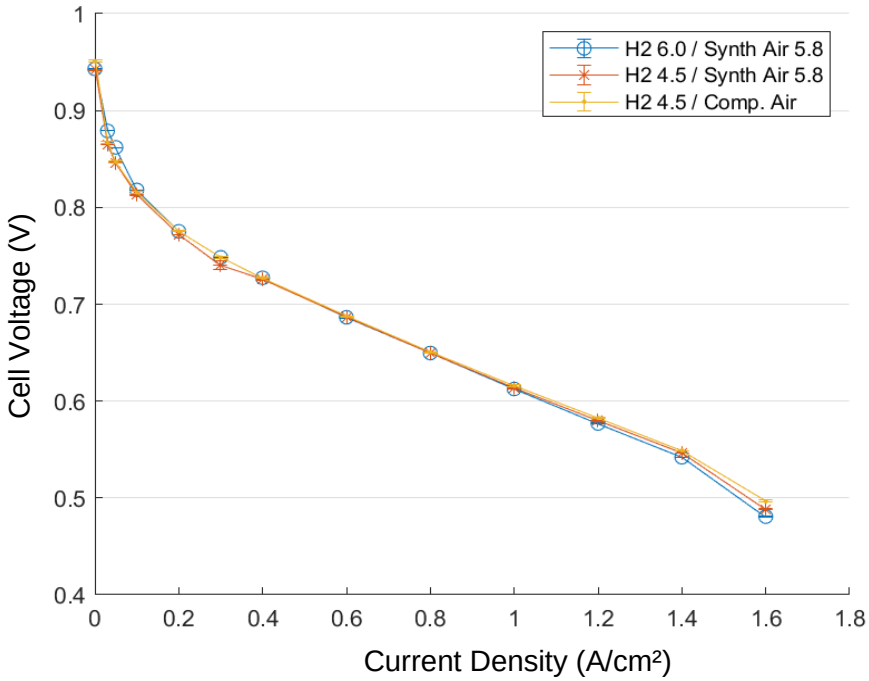

Figure 39 - Polarisation curves at beginning of life for the three gas combinations in CEA reference conditions

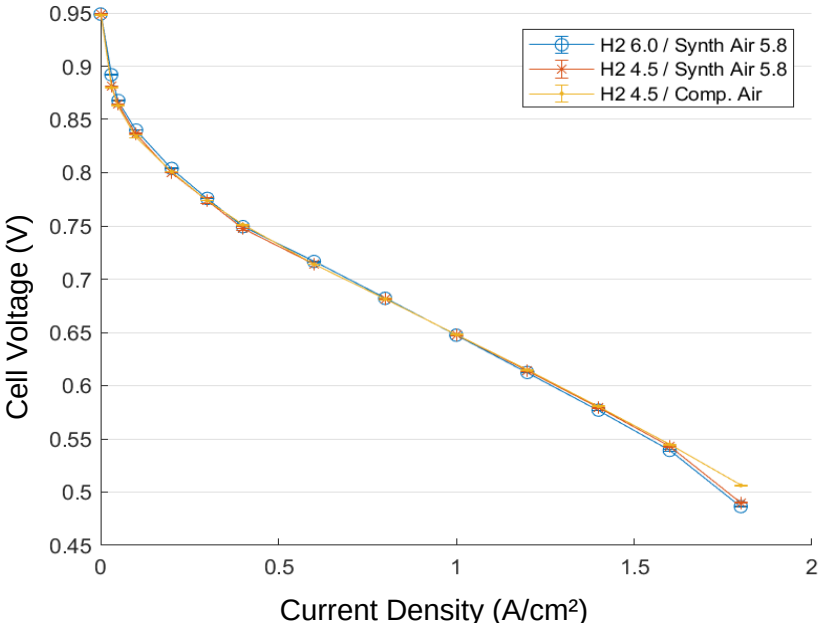

Figure 40 - Polarisation curves at beginning of life for the three gas combinations in ASC conditions

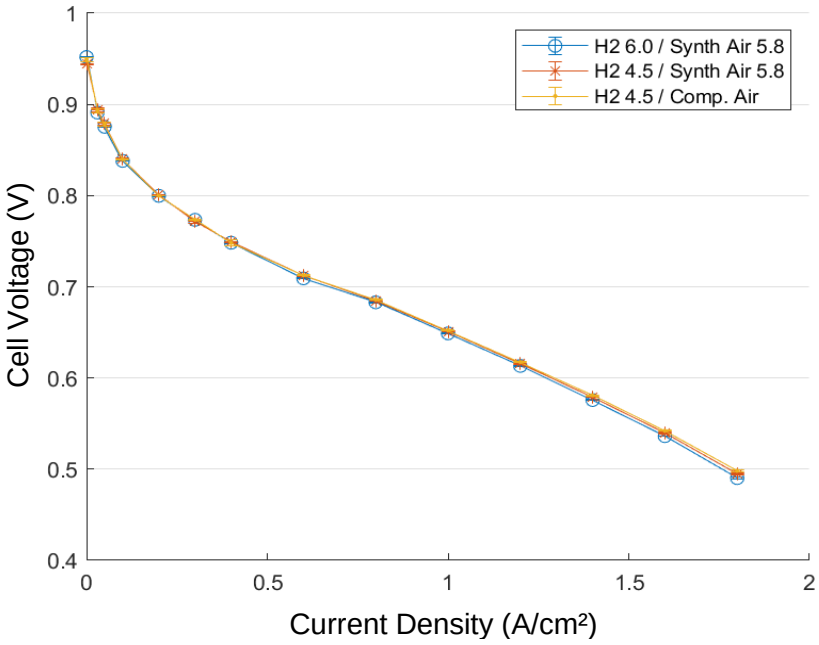

Figure 41 - Polarisation curves at beginning of life for the three gas combinations in EUH conditions

5.2.2 Durability under FC-DLC cycling with different gas compositions

As stated previously, no clear impact is observed between “pure” and “technical” hydrogen or air on the initial performance of the 25 cm² single cell. Nevertheless, the technical grade of reactants may have an impact at longer term (during several hundreds of hours of operation) due to the accumulation of contaminants in the cell. In this section, the effect of hydrogen ain air purity has been studied tage by performing FC-DLC cycles under CEA reference conditions for the different gas combinations.

5.2.2.1 Hydrogen 4.5 + Compressed Air

The data measured during the first FC-DLC aging test using H_2 4.5 and technical compressed air is presented in Figure 42 about the evolution of the cell voltage for each current density step of the FC-DLC cycle over ~ 500 hours. As expected, the higher the current applied to the cell the faster the cell voltage degradation is. The different degradation rates were extrapolated from the linear fitting and represented in Figure 43 and are comprised between 27 and 116 µV/h at OCV and 1.2 A/cm², respectively. This voltage loss is due to the degradation of the cell components and especially the active layer of the MEAs due to the alteration of Pt nanoparticles during FC-DLC cycles. Some degradation is also observed at OCV which may be also due to carbon support corrosion for potential over 0.9 V.

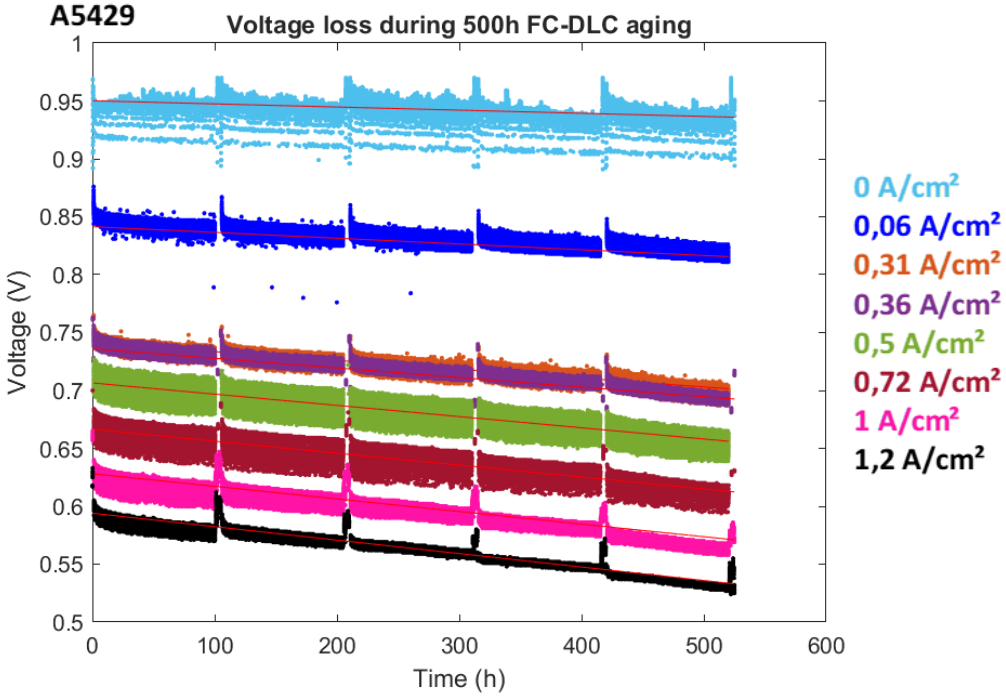

Figure 42 - Evolution of the voltage for each step in the FC-DLC cycle during 500 hours aging. T = 80 °C, RH = 50/50 %, P = 1.5 bar abs (Cell # A5429)

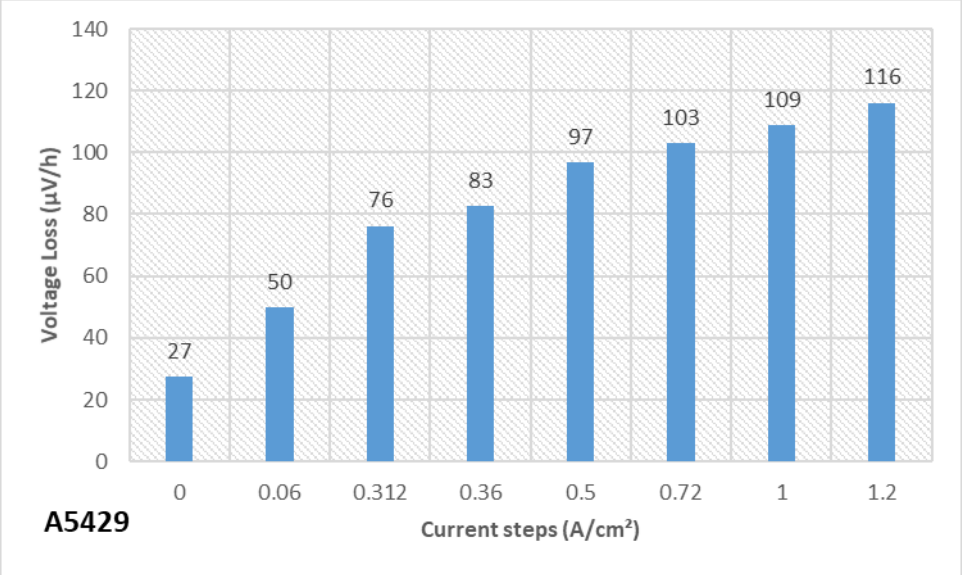

Figure 43 – Degradation rates extracted from the slope of each current density step from Figure 42.

Polarisation curves measured every 100 hours before and after a planned shutdown of the test bench show a rather slow and constant degradation of the cell performance as displayed in Figure 44. The difference between before/after overnight shut-down planned can be used to quantify the reversible degradation of the cell.

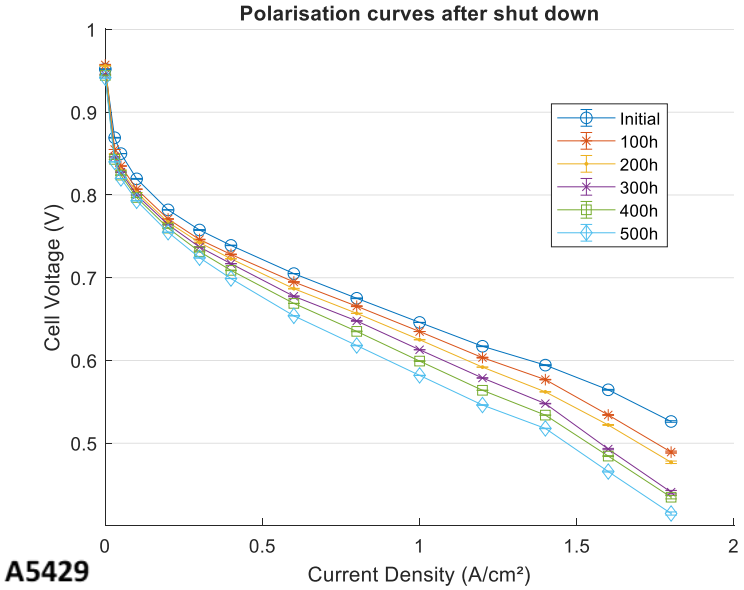

Figure 44 - Polarisation curves controlling the performances every 100 hours during the FC-DLC cycling measured after bench restart at T = 80°C, RH = 50/50%, Stoich A: 1.5 C: 2, P = 1.5 bar abs.

After restarting the bench, the cell shows better performance than directly after 100 h of FC-DLC. This reversible degradations are mainly due to cathode Pt catalyst oxidation, water heterogeneities and possible contamination. Overnight stop followed characterizations cyclic voltammetry makes it possible to remove most of the reversible losses. Figure 45 compares the degradation rates at each current points on polarisation curves. As expected, these values are lower after restart, especially in the medium current density range (0.2 - 0.8 A/cm²).

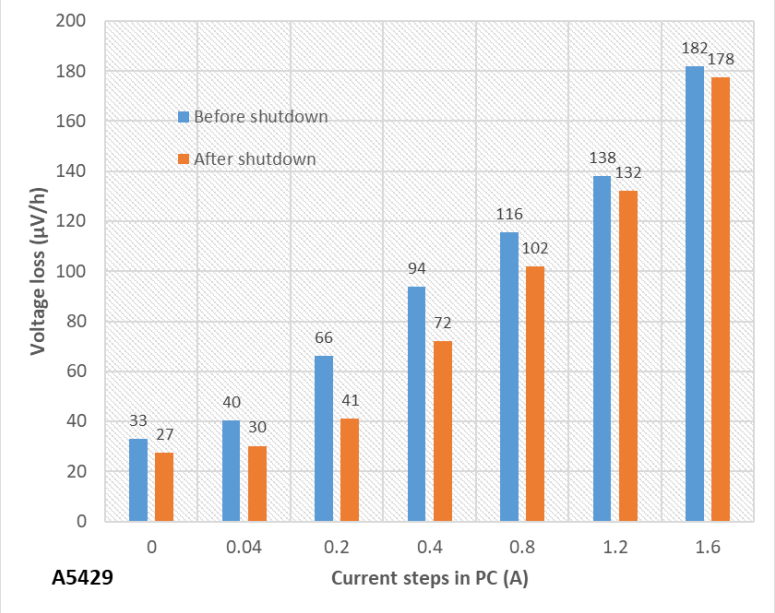

Figure 45 – Degradation rates based on the polarisation curves before and after bench shutdown.

The Electrochemical Surface Area (ECSA) of Pt at the cathode as well as the hydrogen permeation current through the membrane are also measured every 100 hours to monitor the degradation of each component of the MEA. This electrochemical characterisation was performed under the following conditions: H_2/N_2 atmosphere, T = 70 °C; RH = 77 %.

The electrochemical characterisation consists of successive CVs at 50, 100 and 200 mV/s and allows to calculate the ECSA using the proton desorption coulometry. The catalytic roughness (expressed in cm^2_{Pt}/cm^2_{geo}) is then obtained by comparing this Pt ECSA to the geometric active area (25 cm^2). The relative loss of ECSA ($ECSA_t/ECSA_{initial}$) allows to represent directly the percentage loss during FC-DLC aging.

As expected, the ECSA measured at both electrodes significantly decreases during the 500 hours of aging. The raw and relative catalytic roughness on both sides are represented in Figure 13 (a) and (b) respectively. At the end of the test, roughly 40 % of the initial ECSA of Pt is lost explaining the irreversible performance loss observed during the cycling and in the polarisation curves.

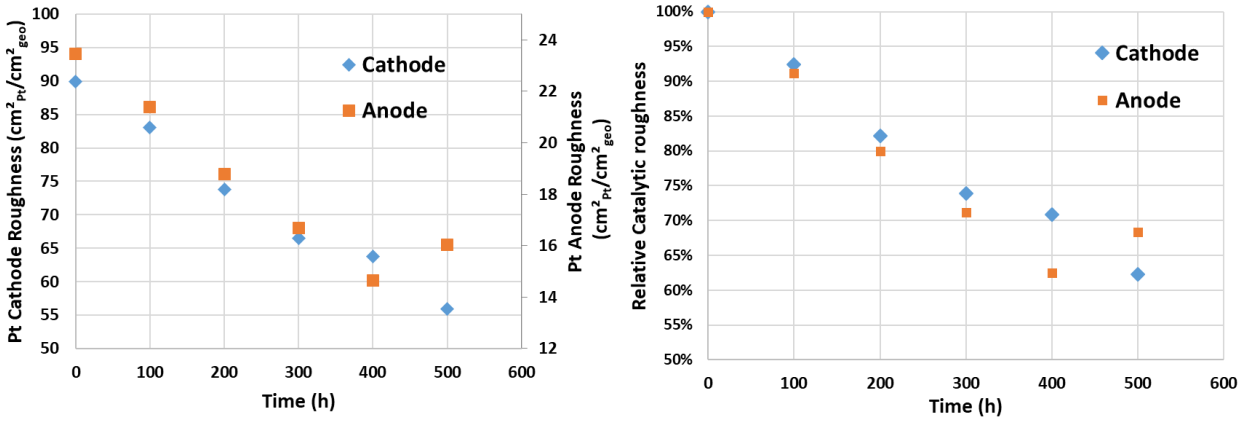

Figure 46 - (a) Raw and (b) Relative Pt catalytic roughness measured at both cathode and anode sides under H_2/N_2 every 100 h during the FC-DLC cycling

The hydrogen permeation current is measured by performing a potentiostatic measurement at E = 0.4 V in H_2/N_2 conditions. Therefore, the hydrogen permeating through the membrane is oxidised and the measured current is characterized every 100 hours for both sides in Figure 47. The small

difference between both measurements might be due to the respective anode/cathode catalyst layer properties. Over the 500 hours of aging, these values remains overall constant meaning that the integrity of the membrane is not affected by the aging and did not form micro pinholes that would facilitate the H_2 crossover.

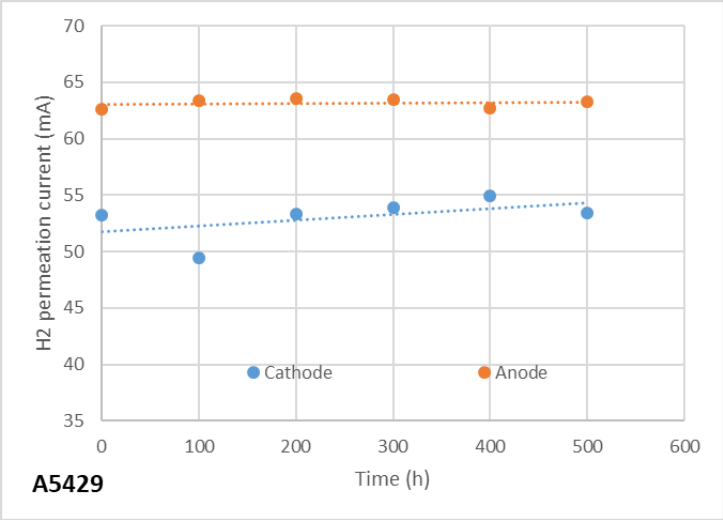

Figure 47 - Evolution of the H_2 permeation current during FC-DLC aging measured under H_2/N_2 at *E* = 0.4 V.

A second reference durability test has been performed using a new MEA (keeping the same cell hardware). In this second test, the maximum current density in FC-DLC has been increased to 1.4 instead of 1.2 A/cm². The durability data are presented in Figure 48.

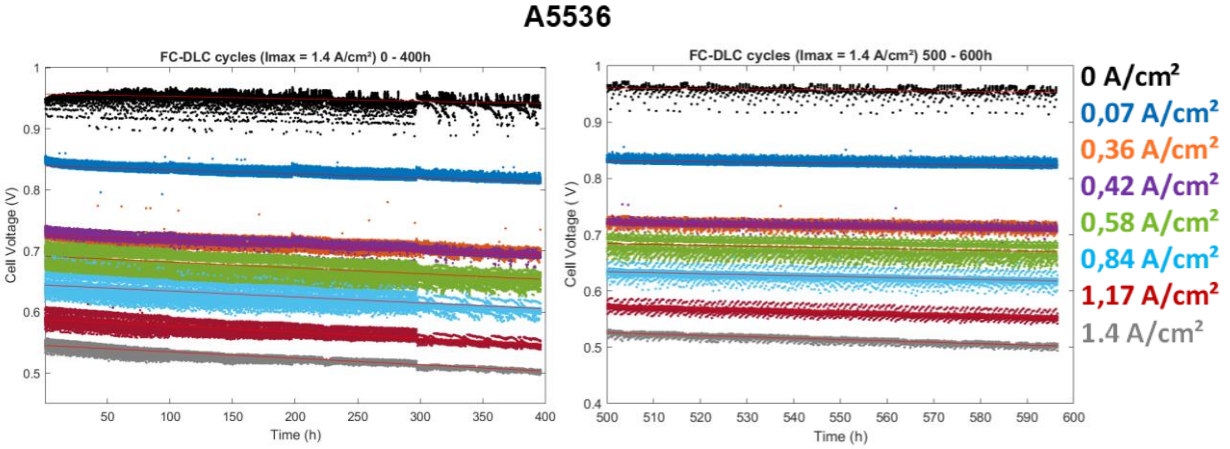

Figure 48 - Evolution of the voltage for each step in the FC-DLC cycle. T = 80 °C, RH = 50/50 %, P = 1.5 bar abs. Left graph presents cycles from 0 h to 400 h and right panel from 500 h to 600 h (Cell reference A5536).

Due to experimental constraints, the bench was stopped between the 400 h and 500 h cycles. This prolonged shut-down phase resulted in a significant recovery of performance. For sake of comparison with the previous aging test, the degradation rates are considering only the first 400 hours in Figure 49. At the maximum current density, the degradation rates based on FC-DLC data are in the same range: 105 µV/h at 1.4 A/cm² and 116 µV/h at 1.2 A/cm².

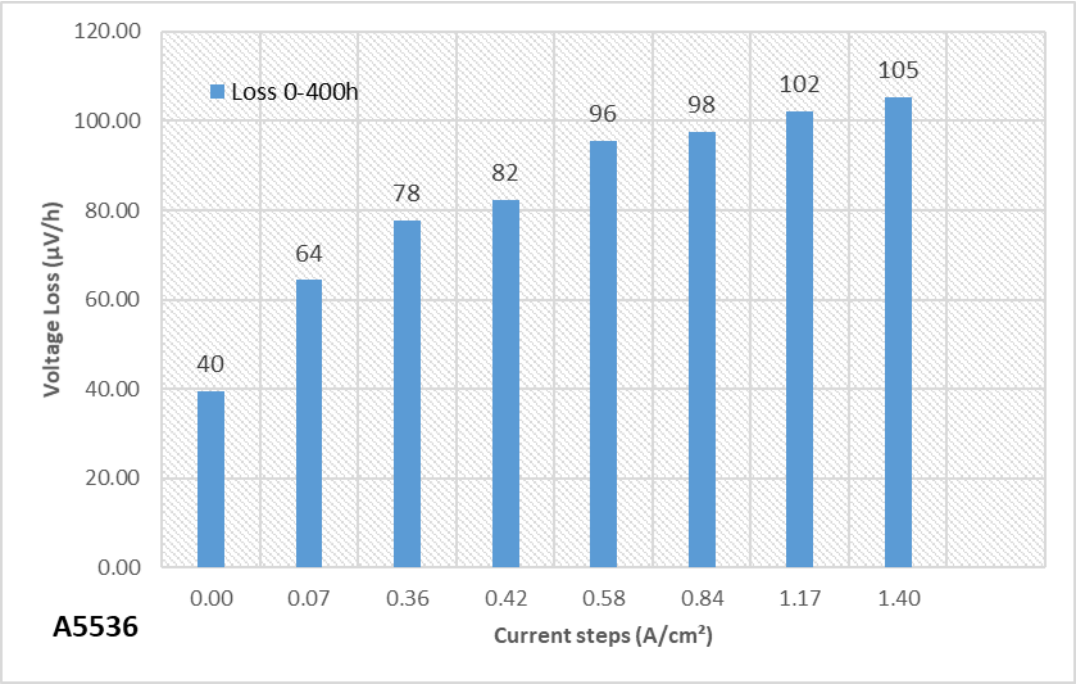

Figure 49 – Degradation rates calculated from the slope of each current density step from Figure 48. (Values considering only the first 400 hours of FC-DLC aging)

The polarisation curves at 100 h, 200 h, and 400 h were not measured correctly due to errors in the script. They are thus not presented in the Figure 50. In addition, as explained previously, the bench was stopped for a long period resulting in a performance recovery for the 500 h and 600 h aging blocks and associated polarisation curves. This results in a series of polarisation curves with missing data. The degradation rate measured on the polarization curves will thus not be calculated for this second test.

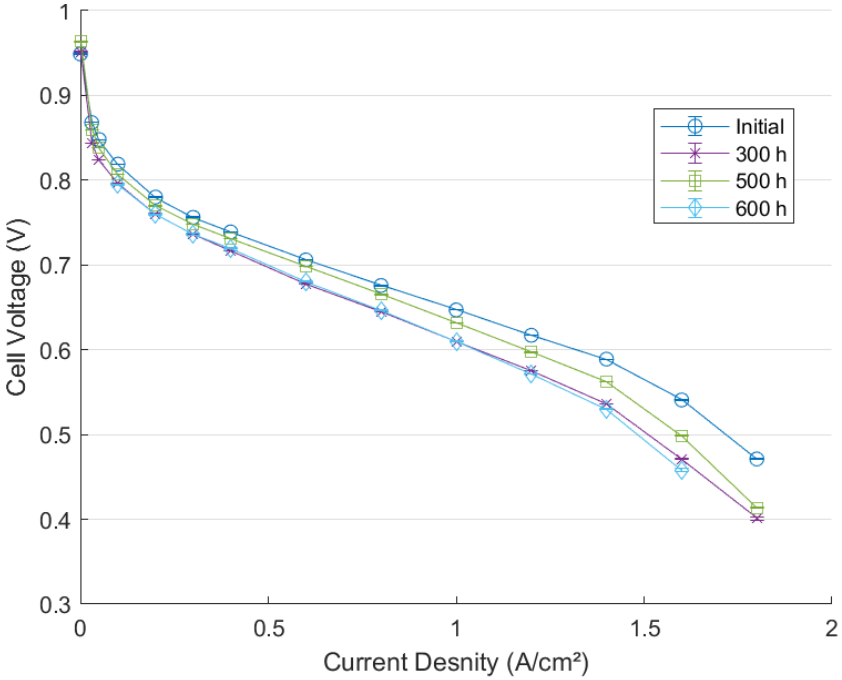

Figure 50 – Periodic polarisation curves controlling the performances each 100 hour during the FC-DLC aging after bench restart at T = 80 °C, RH = 50/50 %, Stoich A: 1.5 C: 2, P = 1.5 bar abs. *The two Pol. Curves at 100 h and 200 h were measured with wrong stoichiometries and the 400 h Pol. Curve was not recorded due to measurement issues.*

Figure 51 shows the evolution of Pt ECSA at the cathode and anode sides. The relative ECSA losses are higher in this second tests (-60 % after 500h vs. -40 % in the first test). This difference remains difficult to explain: it could be due to the measurement uncertainty and/or the higher maximum current (1.4 vs. 1.2 A/cm²) and thus a slightly wider potential range favouring Pt dissolution/redeposition mechanism and Pt nanoparticle growth. Let us stress that the raw ECSA values after 500 h of FC-DLC aging are pretty close between both tests: ~ 60/11 cm^2_{Pt}/cm^2_{geo} (Test #2) *vs.* ~ 65/13 cm^2_{Pt}/cm^2_{geo}.

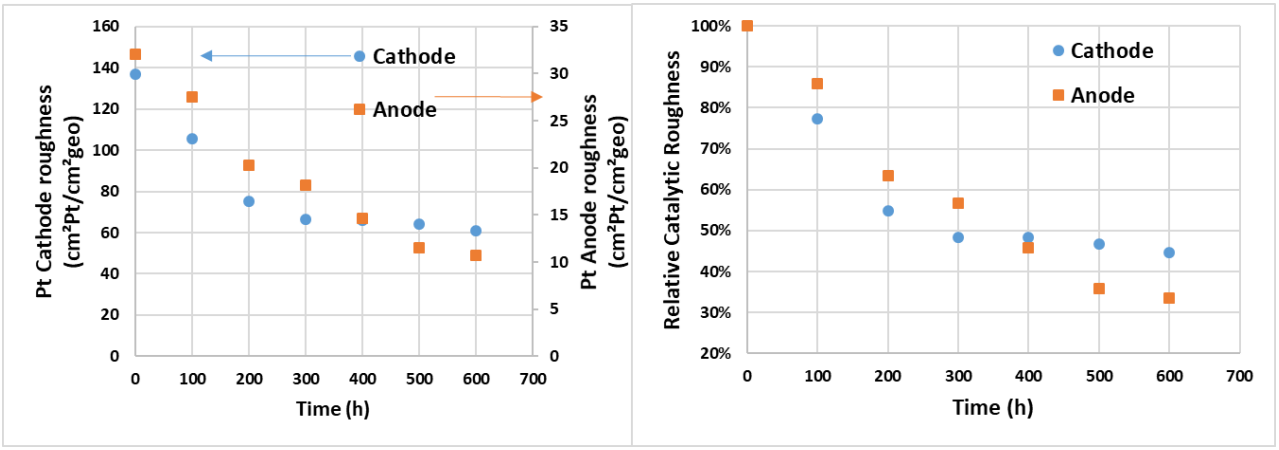

Figure 51. (a) Raw and (b) Relative catalytic roughness measured on both cathode and anode sides under H_2/N_2 every 100 h during the FC-DLC cycling

Regarding the H_2 permeation current in Figure 52, the values are similar between both tests around 2 mA/cm² (see Figure 47 for comparison) and they are also constant during this second test.

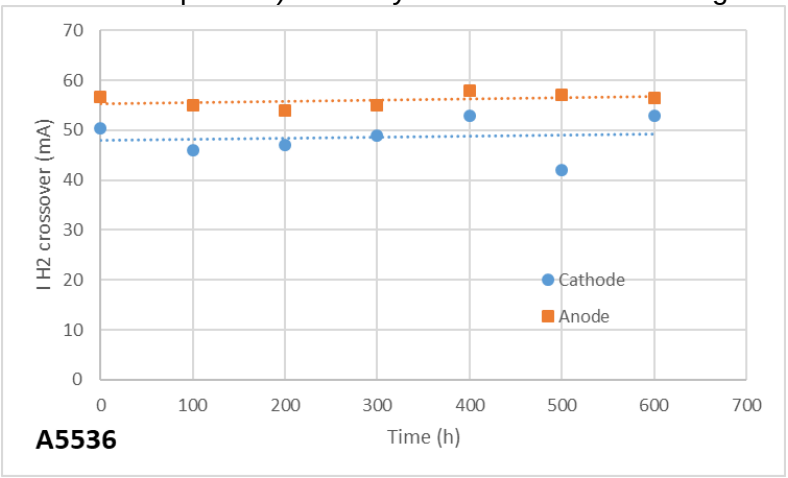

Figure 52 - Evolution of the H_2 permeation current during FC-DLC aging measured under H_2/N_2 at *E* = 0.4 V

On the conclusion, these two reference tests using technical grades for gas purity (H_2 4.5 and technical compressed air) show similar degradation rates during FC-DLC aging which can be used as a baseline when using more pure or contaminated gases.

5.2.2.2 Hydrogen 6.0 + Alternated air purity

In order to quantify the impact of technical air purity on the performance and the durability of PEMFC, a second test campaign has been carried out. Here, 100-hour FC-DLC blocks were applied by alternating synthetic air (N_2 6.0 + O_2 5.8) and technical air.

During the first 600 hours of operation, the two types FC-DLC blocks did not have the same maximum current density value (1.4 with synthetic air and 1.2 A/cm² with technical). This experimental

error was corrected afterwards and the same value (1.4 A/cm²) was applied for the rest of the aging test.
The evolution of cell voltage during this alternated durability tests is presented in Figure 53 and Figure 54. The corresponding degradation rates are illustrated in Figure 55. The evolution of performance during periodic polarization curves between each block is then plotted in Figure 56 and Figure 57.
No significant performance shift can be observed during the alternated blocks and the degradation rates between technical air supply phases and synthetic air supply phases are also very close during the whole test.

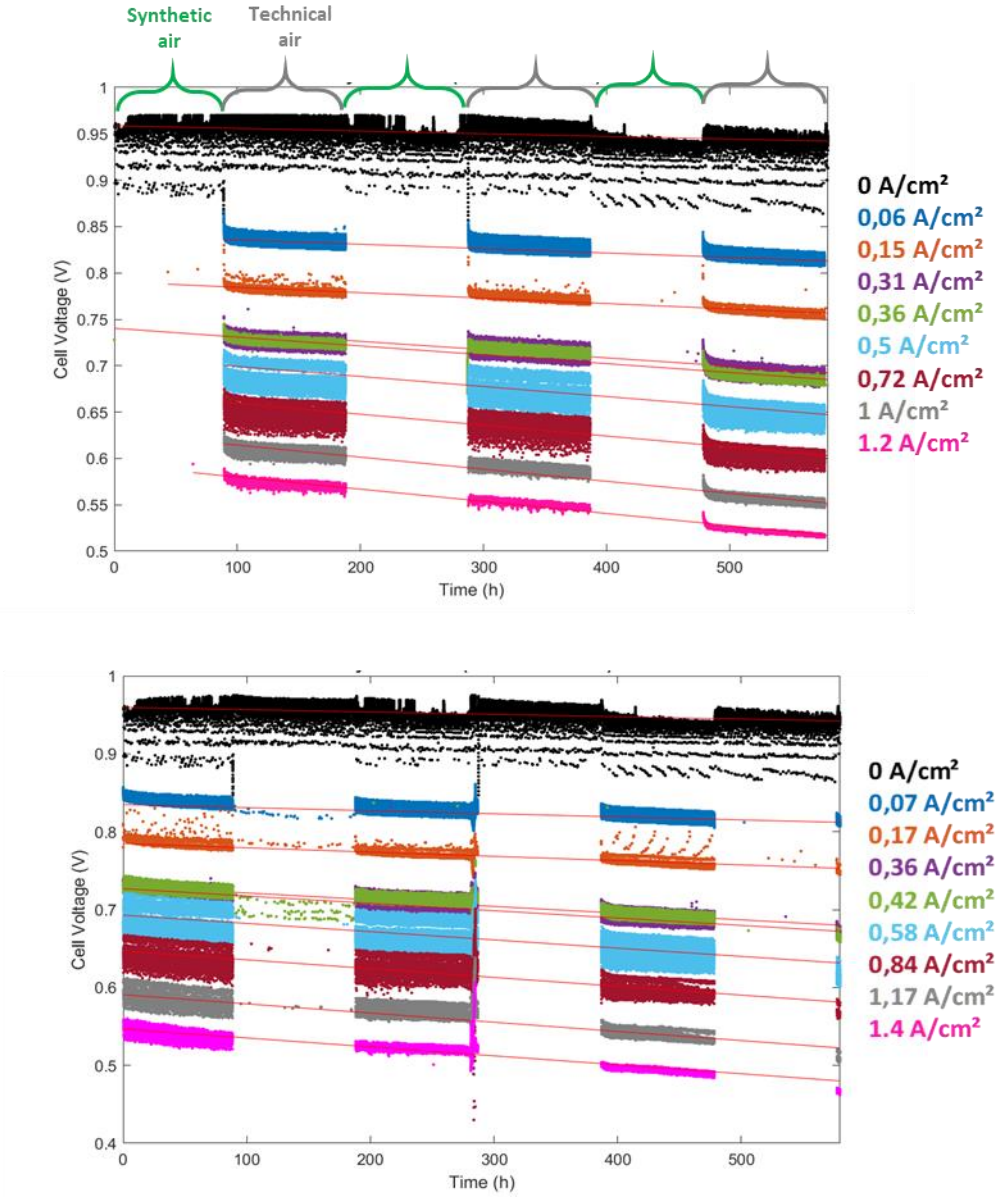

Figure 53 - Evolution of the voltage for each step in the FC-DLC cycles for I_{max} = 1.2 A/cm² (top) and I_{max} = 1.4 A/cm² (bottom) for T = 80 °C, RH = 50/50 %, P = 1.5 bar abs (Cell reference A 5664).

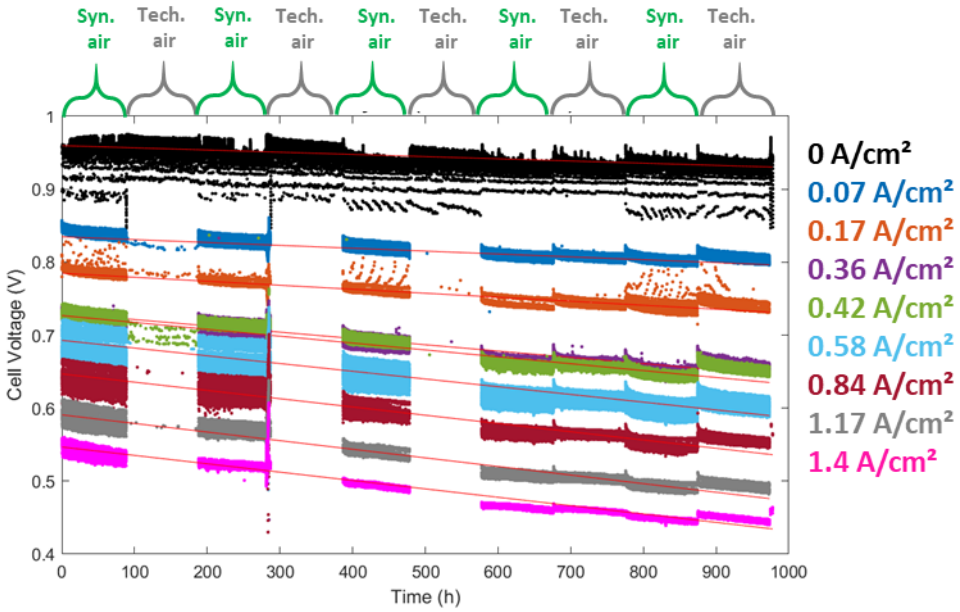

Figure 54 - Evolution of the voltage for each current density step in the FC-DLC cycles. T = 80 °C, RH = 50/50 %, P = 1.5 bar abs (Cell Reference A5664).

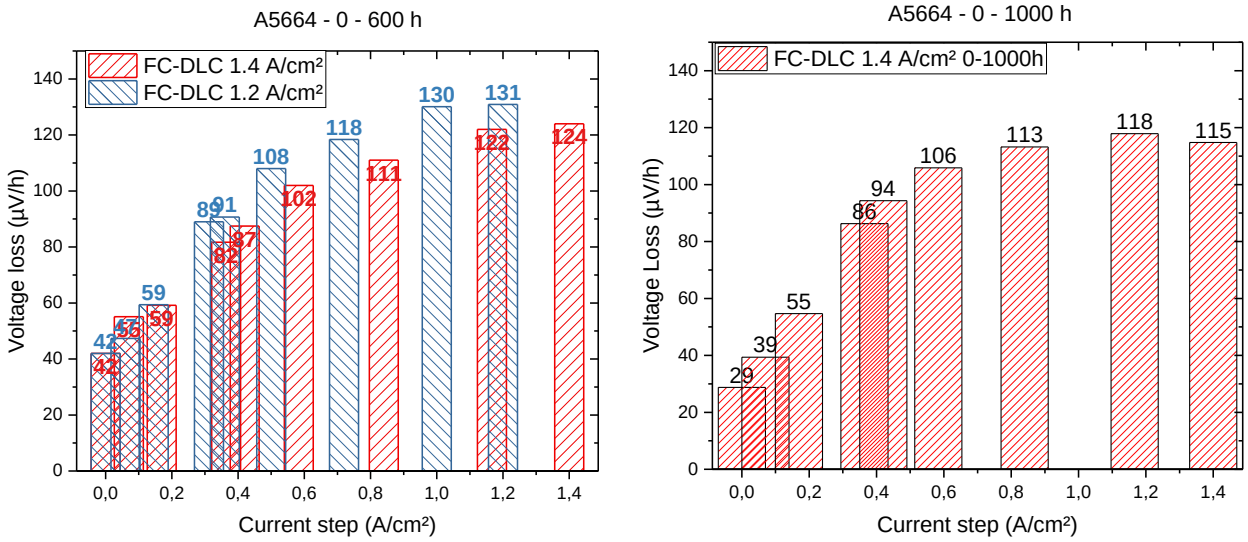

Figure 55 – Degradation rates extracted from the FC-DLC data in Figure 22 and 23. Two slopes were calculated for cycle data with I_{max} = 1.2 A/cm² and I_{max} = 1.4 cm².

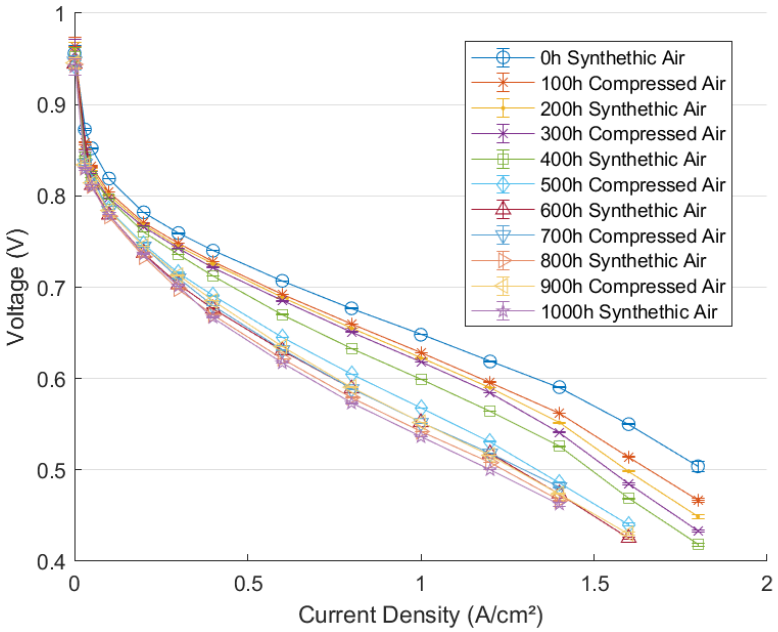

Figure 56 - Polarisation curves controlling the performances, while alternating the air purity every 100 hour during the FC-DLC cycling, measured after bench restart at T = 80 °C, RH = 50/50 %, Stoich A: 1.5 C: 2, P = 1.5 bar abs.

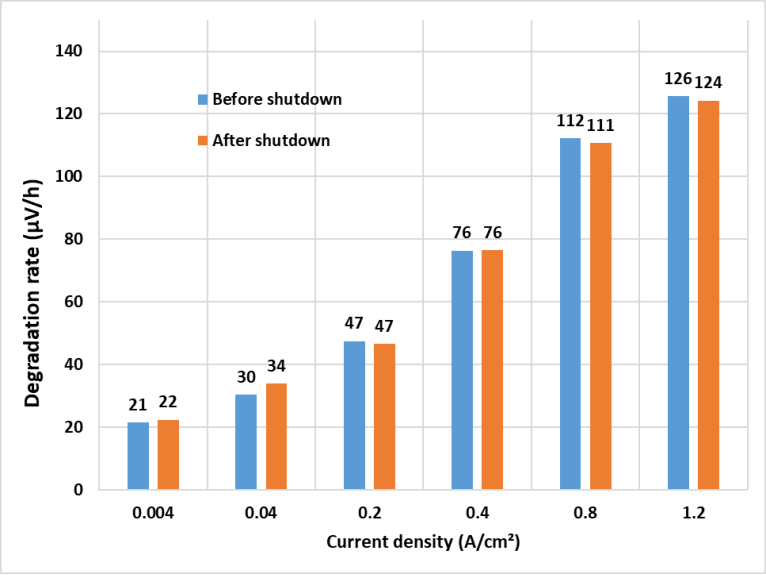

Figure 57 - Degradation rates calculated from the polarization curves before and after bench shut-down.

The evolution of ECSA at both electrodes is presented in Figure 58 and it is also very similar to our previous reference tests. Indeed, the cathode ECSA loss after 500 hours of FC-DLC operation is in the same range as our reference aging using only technical air. Thus, the quality of technical air at CEA seems to be satisfying and does not lead to neither additional performance losses nor additional ECSA losses at both electrodes.

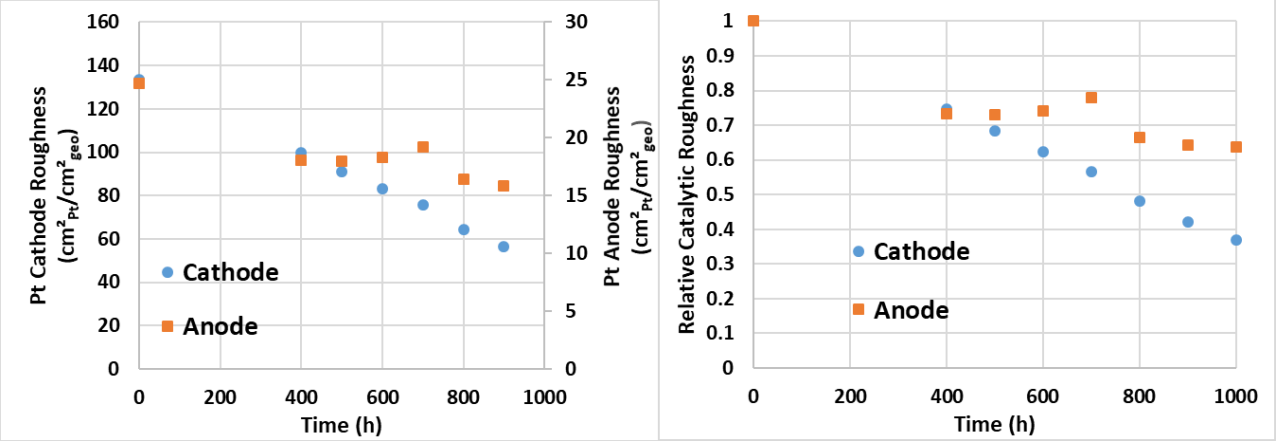

Figure 58 - (a) Raw and (b) Relative Pt catalytic roughness measured on both cathode and anode sides under H_2/N_2 every 100 h during the FC-DLC cycling with alternated air purity (Cell A 5564)

Similarly to our previous reference data, the H_2 crossover through the membrane remains also constant as presented in Figure 59 which attests that the membrane physical integrity is not degraded in this FC-DLC endurance test.

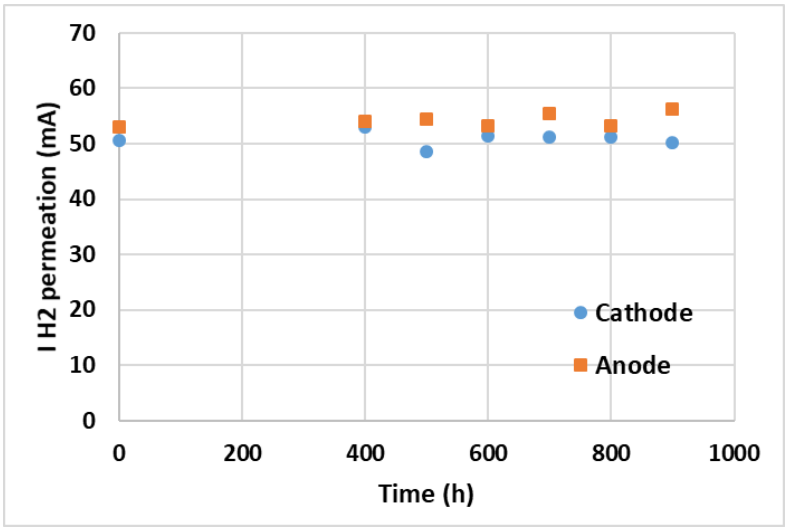

Figure 59 - Evolution of the H_2 permeation current during FC-DLC aging measured under H_2/N_2 at E = 0.4 V

On the whole, PEMFC performance and durability over 1000 hours of FC-DLC cycles measured in single cell are very similar when using “pure” gases (H_2 6.0 or H_2 4.5) as well as technical air or synthetic air (N_2 6.0 + O_2 5.8).

6 Conclusions and summary

The following conclusions can be made from the activities reported from WP3 in A3.1, A3.2 and A.3.3 related to PEMFC testing at both single cell and short-stack levels.

- The proton pump is a robust tool for detecting contaminants in hydrogen at low concentrations owing to its stability under pure hydrogen flow and fast response to contaminant exposure. Additionally, it exhibits good recovery potential.
- On the single cell PEMFC, voltage decay when poisoned at 1 % concentration of hydrogen contaminants was not discernible from the intrinsic decay of the cell when operating with pure hydrogen, within the limits of detection of equipment used and duration of poisoning. On the other hand, 5 % contaminant concentration resulted in an immediate deterioration of the cell.
- The deterioration of ECSA is probably responsible for the degradation of performance of the cell during FC-DLC cycle, particularly at the cathode. No significant difference has been observed between synthetic air (N_2 6.0 + O_2 5.8) and technical air available in the lab during short-term operation (polarization curves) and during long-term durability tests (up to 1000 h of FC-DLC).
- Two identical short-stacks were prepared and tested respectively at CEA and at NPL. Besides, results obtained between both labs are coherent when H_2 + 0.8 ppm CO is supplied.
- Using HYDRAITE and MetroHyve2 feedback and procedures with H_2 recirculation, online CO analysis has been measured in the loop. The results are coherent with the CO-adsorption on Pt active sites (CO values inferior to the CO injected at stack inlet). When a CO-contamination threshold is reached, a sudden increase of CO concentration concomitantly with cell voltage decrease is observed.
- Local current density mapping during 5 ppm CO contamination has been measured. Anode active area located at the H_2 inlet is more severely contaminated and cell operation is shifted towards the H_2 outlet part of the cell.
- Shut-down procedure including air cleaning phase is effective to clean CO poisoning at the anode. This allow to recover reliably the performances and the state of Pt catalytic sites.
- Voltage degradation profiles measured on the short stack PEMFC suggest that the primary cause of performance loss is CO contamination based on the similar decay profiles measured for both the contaminant mixture and single-CO contamination. This could allude to the other compounds in the mixture being adsorbed onto tubing and connection surfaces, thus not significantly affecting the performance of the fuel cell given their low concentration in the mixture. The interactions between all the compounds in the mixture could also potentially result in changes in concentrations or even decay over time.

7 References

[1] X. Zhang *et al.*, 'Influence of Formic Acid Impurity on Proton Exchange Membrane Fuel Cell Performance', *J Electrochem Soc*, vol. 157, no. 3, p. B409, 2010, doi: 10.1149/1.3284646.

[2] A. Talke, U. Misz, G. Konrad, A. Heinzel, D. Klemp, and R. Wegener, 'Influence of urban air on proton exchange membrane fuel cell vehicles – Long term effects of air contaminants in an authentic driving cycle', *J Power Sources*, vol. 400, no. August, pp. 556–565, 2018, doi: 10.1016/j.jpowsour.2018.08.063.

[3] M. A. Schmid, T. Wagner, B. Wiedemann, and J. Scholta, 'Effects of impurities in the cathode airflow on proton exchange membrane fuel cell stacks', *Fuel Cells*, vol. 22, no. 6, pp. 254–270, Dec. 2022, doi: 10.1002/FUCE.202200063.

[4] U. Misz, A. Talke, A. Heinzel, and P. Beckhaus, 'Effects, Damage Characteristics and Recovery Potential of Traffic-induced Nitric Oxide Emissions in PEM Fuel Cells under Variable Operating Conditions', *Fuel Cells*, vol. 18, no. 5, pp. 594–601, Oct. 2018, doi: 10.1002/FUCE.201700214.

[5] U. Misz, A. Talke, A. Heinzel, and G. Konrad, 'Sensitivity Analyses on the Impact of Air Contaminants on Automotive Fuel Cells', *Fuel Cells*, vol. 16, no. 4, pp. 444–462, Aug. 2016, doi: 10.1002/FUCE.201500159.

[6] G. Tsotridis, A. Pilenga, G. Marco, and T. Malkow, *EU harmonised test protocols for PEMFC MEA testing in single cell configuration for automotive applications*, vol. 27632. 2015. doi: 10.2790/54653.

[7] C. Jackson, G. Smith, and A. R. Kucernak, 'Deblending and purification of hydrogen from natural gas mixtures using the electrochemical hydrogen pump', *Int J Hydrogen Energy*, no. xxxx, pp. 1–11, 2023, doi: 10.1016/j.ijhydene.2023.05.065.